EVALUATING THE EFFICIENCY OF A LINEAR BASED ALTERNATOR IN A FREE PISTON ENGINE CONFIGURATION

By

TSHEPO GODFREY KUKUNI

Submitted in fulfillment of the requirements for the degree:

MASTER OF ENGINEERING

IN

ENGINEERING: ELECTRICAL

In the

School of Electrical, Electronic and Computer Engineering

Of the

Faculty of Engineering and Information Technology

At the

Central University of Technology, Free-State

Study Leader: Dr. B. Kotze **Doctor Technologiae: Engineering: Electrical**

Bloemfontein

2018

Declaration of Independent Work

I **TSHEPO GODFREY KUKUNI**, hereby declare that this research project, which has been submitted to the Central University of Technology, Free-State for the degree MASTER OF ENGINEERING in ELECTRICAL ENGINEERING, is my own independent work and complies with the Code and Academic Integrity, as well as the rules and regulations of Central University of Technology, Free-State and that it has not been submitted before to any institution by anyone or me as part of any qualification.

Signature of Student:　　　　　　　　　　　　　　**Date:** May 2018

i

Dedication

I dedicate this dissertation to my late grandfather, Pule John Kukuni, who believed in my educational capabilities and guided me through life.

I further dedicate this dissertation to my beloved grandmother, Mamoitatli Dorcas Kukuni and my parents Monnapule Elby Modise and Pulane Lorraine Modise. Additionally, to both the Kukuni and Modise families as well as my siblings, Matshidiso Evelyn Modise, Madintletse Modise, Rearabetswe Portia Modise and Kgosietsile Modise and my cousin Itumeleng Goodenough Ditlhage, for all the support that they have shown to me throughout the duration of this study.

Ke rata go leboga Thaba-Nchu Circuit`s Vice President, Tshediso Moilwa le President Rev. M. Mokhotsoa mmogo le Selosesha Methodist Church YMG ka dithapelo le di kgothatso tseo bang mphileng tsone gore kebe ke falole dithuto tsaka.

(James 1:5).

Acknowledgements

Abstract

Electrical power generation with minimal negative impact, such as low noise ratio, reduced air pollution and reduced carbon footprint on the environment yet producing high efficiency, has become a goal for numerous research institutes and industries. Therefore, more desirable concept to solve aforementioned problems should be identified and implemented. However, several authors in the field of power generation have identified Free-Piston-Engine-Linear-Generator (FPELG) as a possible solution, due to its advantages, such as high efficiency, minimized volume, fewer frictional losses and reduced carbon footprint, as well as its economic feasibility, as compared to rotary generators with crankshaft mechanism.

Despite the advantages of FPELG over rotary generators, shortcomings of its own were found, such as piston balancing, system combination (linear generator and free piston engine), and stator design, to trap maximum electromagnetism energy, as well allowing smooth piston motion during energy generation. This study investigates this optimal operational efficiency of a FPELG design and development as an alternative electrical energy generation.

The study objective was to evaluate the efficiency of a linear based alternator in a free piston engine linear configuration, with an added necessity to develop a test bench for obtaining the results. Secondly, with this test setup, data was generated scientifically and evaluated to concur that this setup is economical.

Two types of generators (combustion and linear) were designed and built in two platforms. Firstly, the FPELG was physically built and with the same component specifications a Matlab$^{@}$/Simulink program was developed to test the efficiency, voltage, speed and current during the system operation.

Secondly, a combustion engine was developed in Matlab$^{@}$/Simulink for evaluation of the system efficiency as compared to Free Piston Engine Linear Generators. Both engines were examined based on frictional losses to determine which generator is the utmost efficient, compared to the other. Evaluating the assumptions that a linear based alternator in a free piston engine is more efficient were conducted and it was observed that the linear generator is travels at ~2m/s for a cycle of ~ 0.03s.

The speed of the generator depended on the air pressure as well as the load carried by the translator. It was observed that the load mass was exceeding the translator mass and as a result the translator speed was reduced. This caused a bend in the translator and resulted in the translator colliding with the stator.

The magnetic flux depended on the translator speed. However, the Matlab$^{@}$/Simulink showed that the desired output power was feasible with that speed of 2m/s. The physical model also showed that the voltage obtained for all scenarios tested was feasible to meet the expected output power of 7W.

The system efficiency evaluation was based on the frictional losses. The combustion engines results were based only on Matlab$^{@}$/Simulink program. However, it is assumed that the results obtained from Matlab$^{@}$/Simulink program will match the results of the built combustion engines, as is the case for the linear generator.

The combustion engine is seen to experience additional losses, as compared to the linear generator. The losses experienced on the linear generator are lower, due to the fact that FPELG`s have less mechanical wear as compared to the combustion engines.

This research provides a design approach for the alternator, which comprises of the specific measurements for stator design. However, the translator is used as the prime mover between the engine and the alternator. The physical model is then combined into a single unit. Next, the results are simulated and compared to the simulation results from Matlab$^{@}$/ Simulink between the linear generator and combustion engines. The program parameters used for the engine design are relative to the physical model, to compare the results of the same parameters.

Table of Contents

List of Figures

List of Tables

x

Acronyms and Abbreviations

AC   Alternating Current

DC   Direct Current

FPE   Free Piston Engine

FPG   Free Piston Generator

FPLG   Free Piston Linear Generator

FPELG   Free Piston Engine Linear Generator

FPELGM   Free Piston Engine Linear Generator Model

NdFeB   Neodymium Magnets

SmCo   Samarium Cobalt Magnets

Chapter 1: Introduction

1.1. Background to the Fundamental Analysis

In this chapter the background to the study is addressed and the layout of the dissertation is explained. The active power imbalance between generation and loads is caused by insufficient generation, as fuel costs and environmental concerns continue to rise [1]. Furthermore, due to insufficient generation of electricity, the demand for electrical energy is increasing, while the availability of fossil fuels (coal, diesel and petrol) is decreasing [2].

The Free Piston Engine (FPE) concept is defined as a linear crank-less combustion engine, with a linear load directly coupled to the moving piston [3]. However, FPE compared to other combustion engines has the potential to replace the firing cylinder with a variable-pressure bounce chamber and add a control variable to the engine, however, this lead to cost reduction engine power density and higher frictional losses.

However, this concept is introduced as the alternative way for energy generation with reduced carbon footprint. The engine structure consists of two main components, which are the free piston engine and a linear alternator. Compared to combustion engines with a crankshaft mechanism, the combustion process of the free piston linear engine may be optimized through variation of the compression ratio.

The free piston engine linear generator is categorized into three generator types; the single piston, dual piston and opposed piston, of which the dual piston is the one with higher power/weight ratio than others [4].

Emission reduction has encouraged the development of environmentally friendly technology. Free piston engine, coupled with a linear generator and battery, is identified as the promising candidate for high efficiency hybrid vehicles. However, electrical generators with high efficiency and low exhaust emissions are needed for advanced hybrid electric vehicles designs [5].

The linear generator plays a very important role in the free piston engine system for the deliverance of high efficiency system. Electrical generators with high efficiency and low

1

exhaust emissions are needed for advanced designs [6]. As a result, FPE systems have high efficiency and reliability in the energy conversion process as a result of the absence of mechanical devices, like a crankshaft or a connecting rod [7].

Progress in FPE development has not been confined to research laboratories; industries have taken advantage of the mechanically simpler design and lower fuel consumption of FPE [8].

1.2. Problem statement on Efficiency Evaluation Concept

Current research in power generation in a small scale makes mention of a more effective way of generating electricity by means of a linear generator within a free piston configuration.

Evaluating the assumptions stated that a linear based alternator in a free piston engine is efficient, a test bench model will be created to evaluate the characteristics of the aforementioned generator.

1.3. Objectives of the Study

The objective of this study is to evaluate efficiency of a linear based alternator in a free piston engine linear configuration, with an added necessity, to develop a test bench for obtaining these results.

Using this test setup, data is generated scientifically and to be evaluated to concur that this setup is economical.

1.4. Hypothesis

By developing, assembling and building a scaled model of a linear alternator as a test bench, evaluating efficiency compared to readily available combustion engines on the market, with the same output wattage may be conducted and investigated in conjunction with simulations.

Creating a simulation model for evaluating efficiency of a linear alternator using Matlab$^{@}$/ Simulink platform and comparing acquired results to a rotary generator setup of the same wattage.

2

1.5.   Research Methodology

A type of FPE configuration is to be identified, and the design, development and assembly strategy for efficiency evaluation of a linear based alternator has to be implemented. Dual piston engine configuration is identified by previous mentioned literature as the optimal engine configuration, due to lower vibrations and higher power to weight ratio.

Dual piston engine configuration to be assembled, comprises of the built linear alternator, control system and the pistons as indicated in Figure 1.1. A linear alternator is physically built on a small scale, with major components in the same power range as a rotary generator setup.

Efficiency of a linear based alternator is evaluated on both the physical and the simulation models. In addition to efficiency evaluation, multiple graphs may be created illustrating velocity, voltage, current and frictional losses between the two systems. The creation of a simulation model using Mathematical techniques in Matlab$^{@}$/Simulink may determine efficiency evaluation of a linear based alternator in free piston engine configuration.
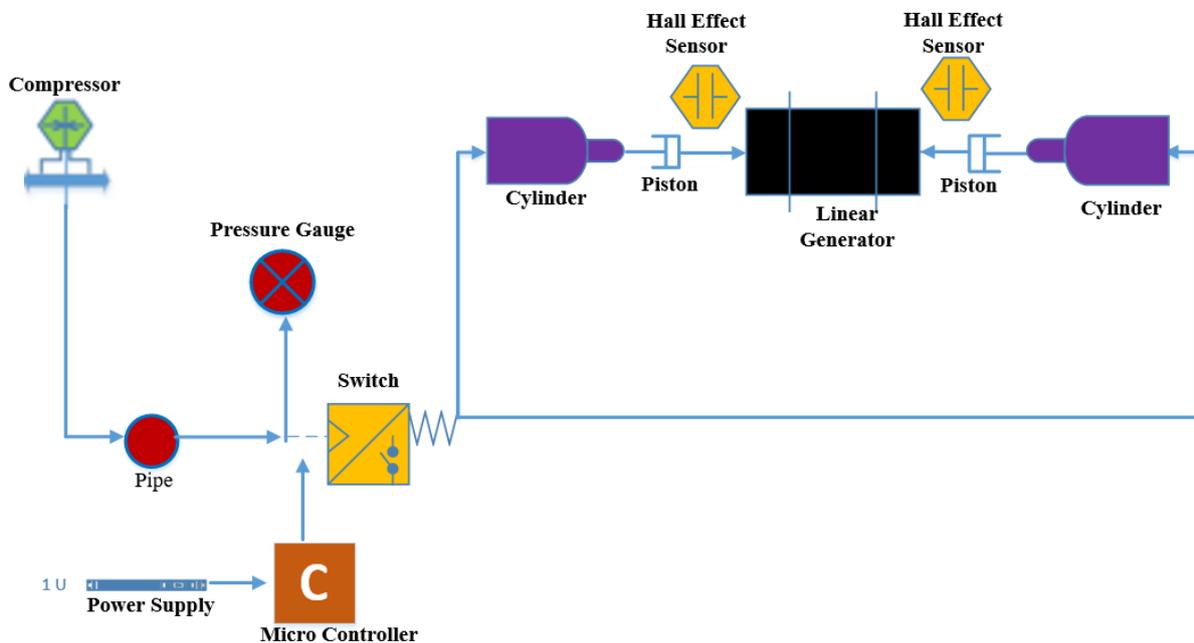
Figure 1.1: Proposed Dual Free Piston Engine Linear Generator Configuration Setup

Figure 1.1 demonstrates the dual piston engine configuration with control system, whereby the cylinder with pistons are operated by air pressure. Once the air pressure is on the control

system from the compressor, the control system will further control the motion of the pistons either to extract or retract within the linear generator through the switch. During that operation the feedback circuit is connected to the oscilloscope to provide the results of system performance in a form of multiple waveforms.

1.6.   Publications and Presentations during the study

During the course of this research work, the following article was presented.

T.G Kukuni, Dr B. Kotze, "Evaluation of a Linear Motor for Utilization in a Free Piston Generator", Southern African Universities Power Engineering Conference, 24-26 January 2018, Johannesburg, South Africa.

1.7.   Layout of the Dissertation

Chapter 1 is an introduction to the dissertation which presents the background, problem statement, objectives of the study, methodology, as well as the hypothesis for the research conducted.

Chapter 2 provides the theoretical overview of the currently available and newly developed linear generators and their applications. The primary focus is based on the materials and concepts needed for designing a linear electrical generator.

Chapter 3 covers the development of the mathematical model, as well as the physical prototype for linear generator system and the mathematical model for crankshaft systems. Matlab$^@$/Simulink library is used to develop the mathematical models.

Chapter 4 discusses the simulation results of both Matlab$^@$/Simulink and the build of a physical prototype model, as well as the crankshaft losses. The proposed system efficiency is evaluated for observation, energy efficiency and to evaluate its readiness for a small production model.

Chapter 5 presents the conclusions and suggests the future works of research to be carried out as to promote efficient linear generator designs within free piston engine configurations.

Chapter 2: Current Developments in Free Piston Generators

2.1.   Introduction

This chapter discusses the theoretical overview of the designs currently available and theoretical simulation model of Free Piston Engine Linear Generators (FPELGs). There are several methods for generating electricity within the FPELG by converting mechanical energy into electrical energy via electromagnetic principles. This chapter is to discuss these options.

2.2.   Literature Review

DC generator usage is restricted, due to low transmission efficiency and high maintenance brushes and commuter segments [9]. In addition to generator history and functionality, the theoretical simulation is presented before the engine design prototype.

Zulkifli et al. [10], discusses the strategy for starting a FPELG, by employing a gas spring of the engine before the combustion that is mechanical resonance and electric motoring, with an open-loop and rectangular current commutation.

The basic model of the FPELG model is implemented to study the efficiency of the linear alternator configuration within the FPE. The equations describing the FPELG development are presented together, with key assumptions for simplicity of the model for use in optimization.

Precise motion control with satisfactory dynamic response, minimal frictional loss and less mechanical wear, are some advantages that linear generators have over combustion engines. Several authors have discussed the use of free piston engine linear generator (FPELG) with an alternator, as the future for powering hybrid cars and for power generation.

This research focuses on evaluating the efficiency of a linear alternator in a free piston engine (FPE) configuration. There are several shortcomings that have been encountered with previous designs of FPELG with an alternator.

6

Famourie et al.., [11], "Design and testing of a Novel Linear Alternator and Engine System for Remote Electrical Power Generation", investigated the stable operation of a spark ignited, gasoline fuelled linear engine and alternator system. His study revealed that at no load, the system was able to operate at 25Hz oscillation frequency and it generated 132 V with an open circuit. Famourie study further states that at a full load, maximum output power of 316 W is produced at 79 V.

Famourie, furthermore, developed two separate systems (alternator and engine), with only a link between two systems being the stroke length and oscillation speed.

Cawthorne, managed to improve Famourie`s design by combining both alternator and engine into a single unit system.

However, Cawthorne`s research did not cover the presentation of speed profiles at various loading levels and examine the efficiency of the various loads at various speeds.

Mikalsen et at.., [12], "A review of free piston engine history and application", indicates that historical free piston engines were mostly of the opposed piston type and had the mechanical linkage between two pistons, in order to balance it and prevent vibrations. Despite all this, they had some advantages over rotational engines and the main advantage was the compactness of the units and the dynamic balance.

Patrichencko el at.., [13], the authors, present an "Approach to controlling the extreme positions of a free piston generator using linear electric machine". The machine is used to provide the appropriate compression ratio necessary for ignition and limit the stroke of the piston in the expansion phase, using Matlab® /Simulink platform for the model implementation.

Furthermore, Ferrari el at.., [14], "Development of a free piston linear generator for use in an extended range electric vehicle", presents the methodology of the free piston engine linear generator. The authors present the use of the FPELG as a range extending device in an electric vehicle to achieve the robust operation of the FPLG system, hydraulic actuator implementation for FPLG motion simulation had to be developed.

A simulation program may be created for efficiency testing at the desired frequency and for motion control of the FPELG on a platform like Matlab®/Simulink. The design, simulation and implementation of free piston engine linear generator as an alternative means of energy supply can be created and developed.

Previously developed FPELG with Alternator research, focused on hybrid vehicles and environmental concerns, however, this research is based on utilizing linear alternator in a Free Piston Engine configuration as a possible alternative energy solution by evaluating the efficiency of the linear alternator.

However, determining the number of turns is important when building any type of generator. A new winding design affects other parameters, such as resistance and inductance. This results in copper resistance changing due to its relation to resistivity and length and area of the wire as indicated in the formula below:

$$R_{arm} = \frac{Q_{cu}*l}{A} \qquad (2.1)$$

Where: R_{arm} = Copper Resistance, Q_{cu} = Resistivity of the copper conductor,

l = Length of the wire, A = Cross- Sectional area of the wire [15].

The number of windings further causes a change in inductance, since inductance depends on magnetic flux through a coil of a given number of turns and current is linked by the coil.

$$L = \frac{N\emptyset}{I} \qquad (2.2)$$

Where: L = Inductance, N = Number of turns in the coil, $\emptyset$ = Total magnetic flux, I = current.

Equation 2.2 can be simplified and re-written as follows:

$$\emptyset = \frac{NIA}{l} \qquad (2.3)$$

Thus, introduction of equation (2.4) where:

$$L = \frac{N^2 A}{I} \qquad (2.4)$$

Equation (2.5) can be introduced into equation (2.4), by making inductance subject of the formula in equation (2.2), which therefore results in equation (2.5) as follows:

$$\emptyset = \frac{NIA}{l} \qquad (2.5)$$

Linear machines that are recently being manufactured and designed, usually brushless linear generators. Commutation is performed electronically using electric switches and other forms

8

of sensors that provide logic signals for commutation. Tubular or cylindrical linear generators as indicated in Figure 2.1, are the type of generators that are being constructed.
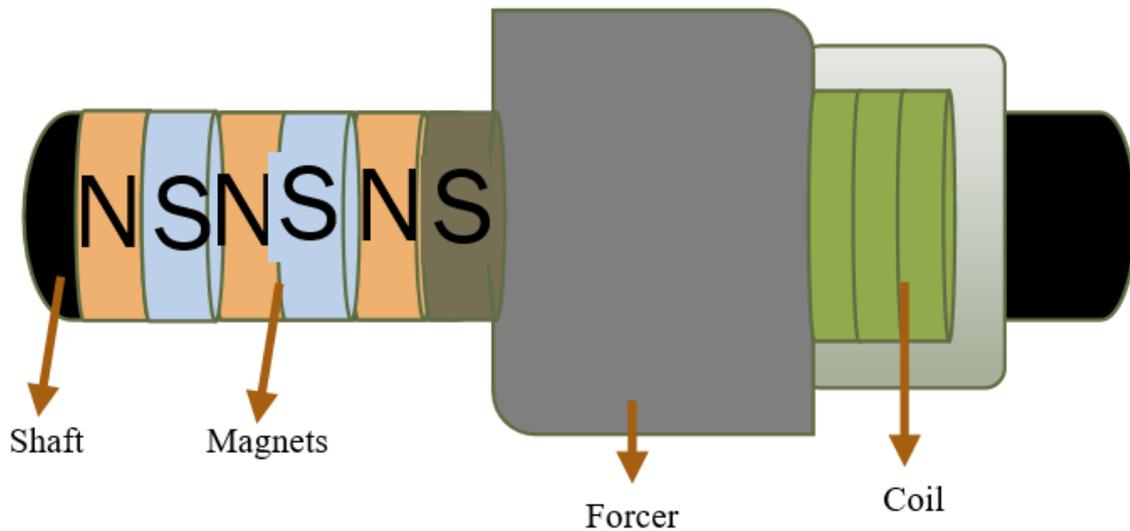
Figure 2.1: Cylindrical Linear generator with circular magnets on a shaft and a force with coils [15]

The design is similar to the linear actuator while the difference being that magnets or coils are repeated to increase the stroke length. This design may have magnets on the inner tubular housing or on the shaft [16].

Concentrated windings, as shown in Figure 2.1, have benefits over traditional distributed windings in-terms of lower resistance windings and a higher slot fill factor [17]. Furthermore, concentrated windings also provide higher inductance, which is advantageous when designing for a wide speed range [18].

$$\eta = \frac{P_{out}}{P_{in}} * (100) \qquad (2.6)$$

Where:

η denotes efficiency,

P_{out} = Output Power,

P_{in} = Input Power.

$$w = F * D \qquad (2.7)$$

9

w denotes work done, F denotes force and D denotes displacement between two pistons, however, from equation (2.7) we can derive equation 2.8 by adding the following equation:

$$v = \frac{D}{t} \tag{2.8}$$

However, equation 2.8 can be simplified into

$$D = vt \tag{2.9}$$

Which therefore introduces the t time factor in equation 2.10 as follows:

$$P = \frac{w}{t} \tag{2.10}$$

Where: P denotes power,

w is the work done,

t is the time,

v is velocity,

2.3. Free Piston Engine development

For any research to accomplish accurate desired results, the fundamental principle is to identify the simulation or physical models to be developed. However, for this study a Free Piston Engine Linear Generator Model (FPELGM) developed consists of combustion cylinder, linear alternator and control system.

In the current designs, the load on FPELG is connected after the rebound devices for a single piston FPELG configuration to act as a storage device. Nemecek et al. [19], describes the Free Piston Generator Model (FPGM) and its control for achieving steady operation, by highlighting the piston acceleration engendered by combustion mixture and how the energy is released in opposite cylinders as in indicated in Figure 2.2 below:
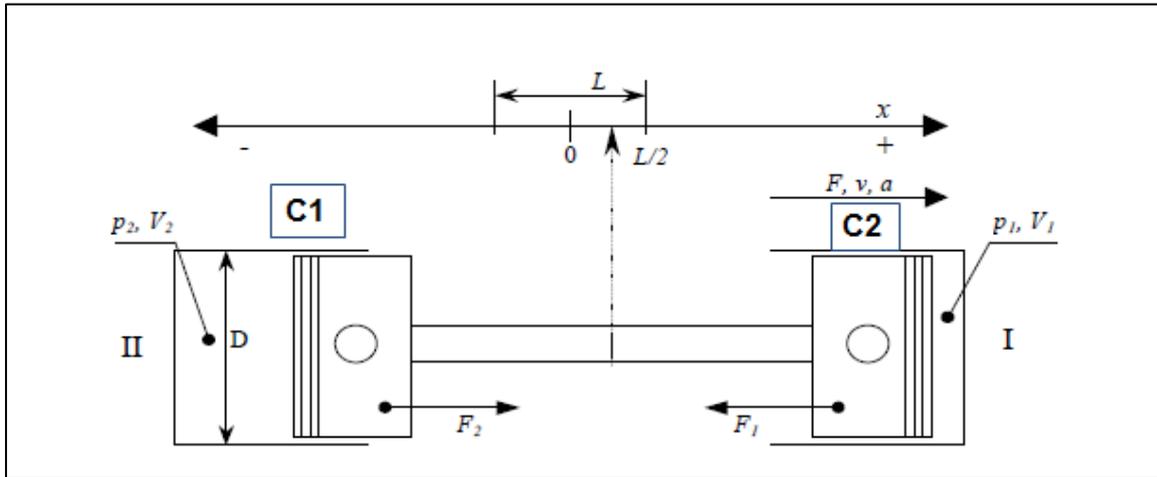
Figure 2.2: Simplified FPG diagram constants and variables [18]

The following equation is aimed at presenting the mathematical representation of Figure 2.2, where both pressure, density and velocity are expressed, as well as their effect on the system performance.

$$p_1 - p_2 = \frac{1}{2}\rho(v^1{}_1 - v^2{}_2) \tag{2.11}$$

Where:

p is pressure,

ρ is the density,

v is the velocity.

11

The air pressure is applied to the one side of the chamber (C1) and the piston extracts F1 to the second chamber (C2), where F2 retracts the load through the linear alternator.

The Free Piston Engine (FPE) is a machine that employs pistons, which are dynamically coupled to energy storage and absorbing devices, to convert thermal energy into useful form such as electricity [16].

The configuration illustrated in Figure 2.2, apart from demonstrating acceleration caused by combustion mixture further highlights a single piston with load directly attached to the opposite piston.

Air pressure is one the fundamental basis in the current engine design concept, where the force balance equation for dual piston linear engine is described by authors of Ref [19] as follows, due to the fact that the engine cannot start operating without the air pressure force application.

$$P_L(X_p)A_B - P_R(X_p)A_B - F(X_p) = m\ddot{x} \tag{2.10}$$

Where:

$P_L(x)$	Pressure in the left cylinder,
$P_R(x)$	Pressure in the right cylinder,
A_B	Bore Area,
F(x)	Electromagnetic and friction force,
m	Mass of the translator,
X_P	Translator position,
$\ddot{x}$	Displacement of translator.

However, for this research other forms of frictional losses are not accounted for and are assumed to be constant and only bearing frictional losses are accounted for, due to the advantage of a linear generator with a free piston engine having reduced frictional losses associated with crankshaft mechanism as compared to combustion engines [19].

The concept of reduced frictional losses within a FPELG, will be investigated as to compare the losses that occurs between FPELG and rotary generators, bearing in mind that this research is focused on efficiency of the system based on the losses.

The translator motion is initiated by the reciprocating motion of both the left and right cylinders. However, the motion of the pistons is opposite, meaning that the time in which the left cylinder retracts, and the right cylinder expands and vice versa.

For the present study, the cylinder volume is obtained by assuming that at the midpoint, where $x = 0$ is known, the assumption may be made by equating the cylinder pressure and cylinder volume of the one cylinder to be equal to the pressure and cylinder at the focal point as follows:

$$P_R V^n{}_R = P_m V^n{}_m \qquad (2.12)$$

However, equation 2.12 can be substituted into equation 2.13 and result in

$$P_R = P_m \left(\frac{V_m}{V_R}\right)^n \qquad (2.13)$$

Where:

V_m = Cylinder Volume at the focal point,

V_R = Right Cylinder volume,

P_R = Pressure at the right cylinder,

P_m = Cylinder at the midpoint,

n = ratio.

R in the equation, solely represents both the left and right cylinder, however, for the complexity of the equation only one side of the system is used on the above equations.

M is the midpoint of the system between the two cylinders.

Bearing in mind that these equations further apply on the left cylinder, by reason of the dual air pistons that are used; therefore, the equation is within both cylinders. However, for this study, the heat factor is not a phenomena accounted for during the operation, but rather the air pressure is accounted for, since it plays a huge role in the motion of both air pistons. Since combustion occurs at a constant volume the following equation is derived.

However, midpoint volume V_m can be expressed as follows:

$$V_m = \left(\frac{\pi b^2}{4}\right)x_m \tag{2.14}$$

Where:

b   cylinder bore

X_m *translator position*

The movement of the piston assembly is decided by forces acting on it, while the generator is in a stable state. In Figure 2.3 below, Miao et al., [20], demonstrates how forces act on the piston assembly of FPELG.
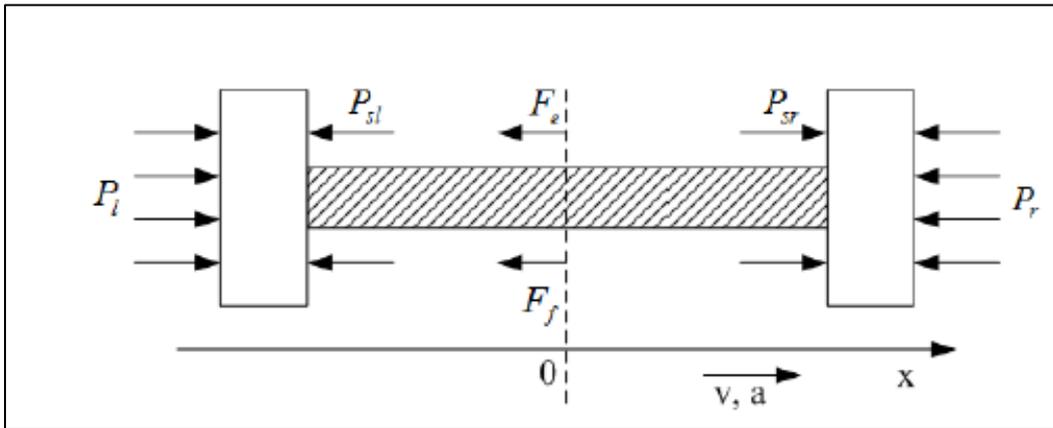
Figure 2.3: Forces acting on the piston assembly of the FPELG *[20]*

The following equations demonstrates the operations that occur on Figure 2.3, during scavenging process of the FPELG.

$$(P_l - P_r)A - F_e - F_f = m\frac{d^2x}{dt^2} \tag{2.15}$$

Where P_l = In cylinder gas on the top surface of the left cylinder,

P_r = In cylinder gas on the top surface of the right cylinder,

A = Area of the piston,

F_e = Electromagnetic force caused by the load,

F_f = Frictional force,

M = Mass of the piston assembly including the translator,

14

x = Piston displacement,

t = time.

However, as indicated in Chapter 1, other forms of frictional losses are not accounted for, apart from frictional losses in this research, as linear generators within a free piston engine primary objective is to illuminate the crankshaft mechanism and to reduce frictional losses within a constructed alternator.

2.4. Free Piston Engine Model

The Free Piston Engine can be configured in three different forms as illustrated on Table 2.1 below. The piston forms illustrated highlights the opposite piston, single piston and dual piston configuration.

Table 2.1: Typical free piston engine configuration *[21]*.

Type	Representation	Comments
Opposed Piston		Intrinsically balanced and vibration-free when the pistons have equal masses; piston synchronization is required.
Single Piston, Dual Combustion Chamber		Every oscillation is a power stroke—potentially greater efficiency. Unbalanced and possibly difficult to control.
Single Piston and Combustion Chamber		Simple and easy to control, but it is unbalanced. Counterweights may be used.
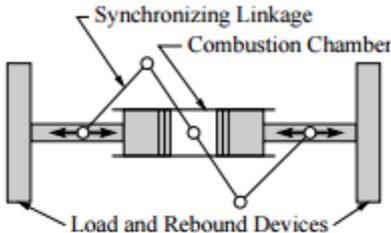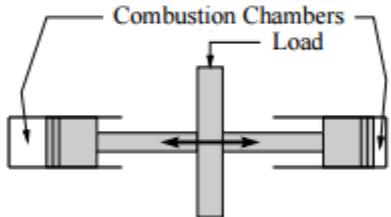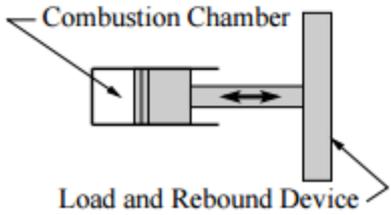
15

Since the focus based on a dual piston engine linear alternator is studied, coupling of the load in FPE is the key to understanding the design and functionality of the engine.

It is critical when evaluating engine efficiency to accurately place your load at a more convenient place where the load will not have any negative impact on the operation of the engine, by reducing speed at which the pistons are travelling. The general load acting on the engine is preferably coupled to the linear alternator and not the engine pistons. However, Aichlmayr [21] states that it is still possible to place the load on the pistons, provided that the opposing piston is synchronized with the motion of the extracting piston, to prevent collision and keeping the loads small. Aichlmayr`s research is further supported by Junkers.
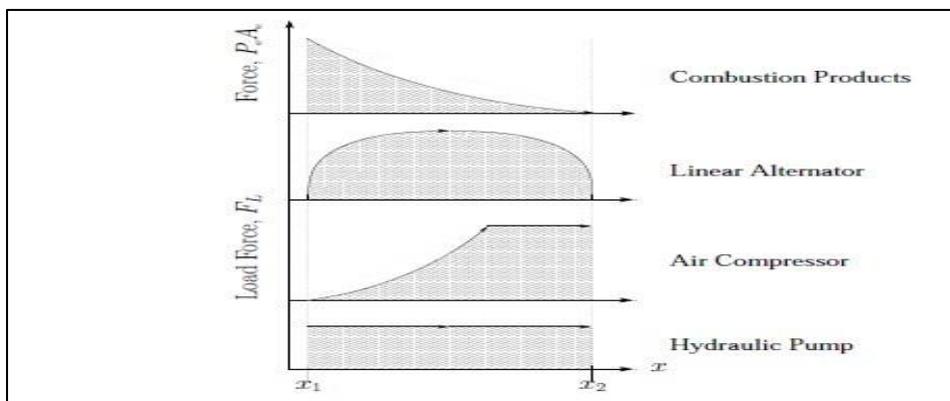
Figure 2.4: Load compatible with FPE *[21]*

2.5. Solenoid Selection

Solenoid copper wire is one of the fundamental components to be used for this research when developing a linear alternator. However, for every output required it is important to know the wire gauge of the copper wire to avoid burning the wire and effectively obtain the desired output. Table 2.2 below displays the American wire gauge used for solenoid copper wire selection.

Table 2.2: American Wire Gauge *[22]*

AWG Gauge	Conductor Diameter (Inches)	Ohms per 1000 ft (Ω)	Ohms per km (Ω)	Maximum amps for chassis wiring (A)	Maximum amps for power transmission (A)	Maximum frequency for 100% skin depth for solid conductor
0,000	0,460	11,684	0,049	380	302	125
0,00	0,410	10,403	0,061	328	239	160
0,0	0,365	9,265	0,077	283	190	200
0	0,325	8,252	0,098	245	150	250
1	0,289	7,348	0,123	211	119	325
2	0,258	6,543	0,156	181	94	410
3	0,229	5,826	0,197	158	75	500
4	0,204	5,189	0,248	135	60	650
5	0,182	4,620	0,313	118	47	810
6	0,162	4,114	0,395	101	37	1100
7	0,144	3,665	0,498	89	30	1300
8	0,129	3,263	0,628	73	24	1650
9	0,114	2,905	0,792	64	19	2050
10	0,102	2,588	0,998	55	15	2600
11	0,091	2,303	1,260	47	12	3200
12	0,081	2,052	1,588	41	9,3	4150
13	0,072	1,828	2,003	35	7,4	5300

2.6. Control Systems

Petrichenko et al.., [13], use the principles of thrust control for electrical drive. Since the control system is based on FPE, the positioning of the piston is external due to the fact that they are attached to the shaft inside the linear alternator.

However, Kolpakhchyan et al.., [23], introduces the use of pulse width modulation (PMW), to determine the required winding current value.

Kolpakhchyan et al.., further, proposed the control systems structure based on the principles of descendant control, as in Figure 2.5.

17
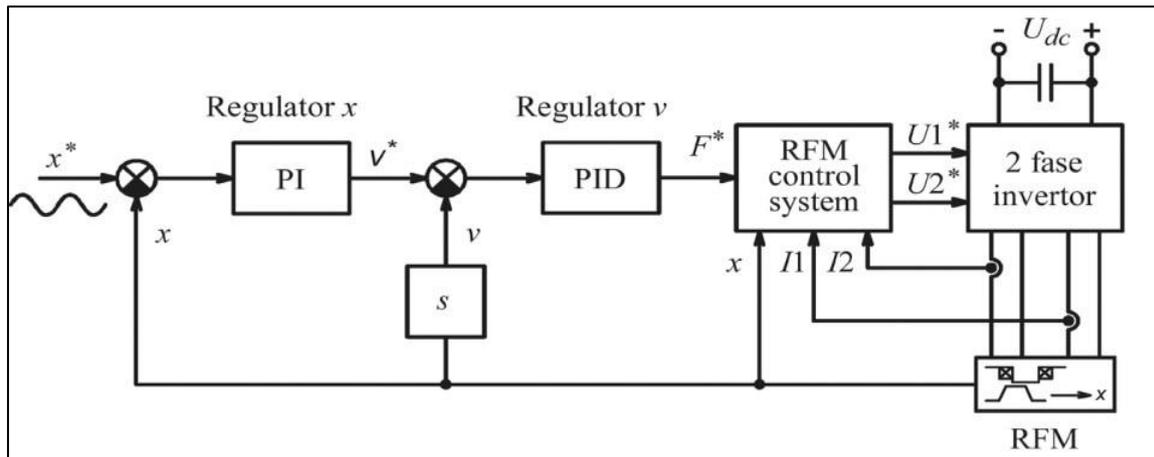
Figure 2.5: Control System structure *[24]*

For this research, since piston control is accounted for by the fixed attachment on the shaft, the losses that occur during the cycles are taken as calculation basis, due to the cylinder pressure. The piston motion as well as the speed profiles are based on the control system in relation with the supply frequency.

2.7. Magnetic Properties

The selection of magnets is important in a generator design, since it is significant to know the magnet`s capabilities, such as energy and mechanical strength etc. Several authors agree that neodymium permanent magnets are the leading choice for FPELG design as indicated in the Table 2.3 below:

Table 2.3: Permanent magnet material comparison

Properties	Lowest	Low	High	Highest
Cost	Ferrite	AlNiCo	$Nd_2Fe_{14}B$	SmCo
Energy	Ferrite	AlNiCo	SmCo	$Nd_2Fe_{14}B$
Operating Temperature	$Nd_2Fe_{14}B$	Ferrite	SmCo	AlNiCo
Corrosion Resistance	$Nd_2Fe_{14}B$	SmCo	AlNico	Ferrite
Resistance to Demagnetization	AlNiCo	Ferrite	$Nd_2Fe_{14}B$	SmCo
Mechanical Strength	Ferrite	SmCo	$Nd_2Fe_{14}B$	AlNiCo
Temperature Coefficient	AlNiCo	SmCo	$Nd_2Fe_{14}B$	Ferrite

Mahadi et al.., [25], states that for permanent magnet selection, several magnetic properties are the important parameters that need to be observed, before a magnet could be used, which is flux density, coercive force and maximum energy product. These parameters determine the performance of the permanent magnets and NdFeB magnets with N30EH grade are the leading magnets for linear alternator.

Callahan [26], supports Mahadi`s observation stating that NdFeB magnets are the leading candidate magnets for generator modelling. However, these materials are difficult to utilize with temperatures over 100ºC, hence in the "*properties of NdFeB magntes*" in Table 2.4, the selected operational temperature is picked at 80ºC, treated as the maximum operating temperature for this study.

Mahadi et al.., "Thermal analysis of a neodymium iron boron (NDFEB) magnet in the linear generator design "further proved their observations of NdFeB as the best and reliable permanent magnets for use in linear generators.

Mahadi [27], further supports their statement by introducing Figure 2.8, which illustrates the demagnetization curves as a function of temperature.

The main linear generators types are as follows:

- Moving Iron – the heaviest linear generator configuration.
- Moving coil – allows the coil to create power during scavenging.
- Moving magnet – used in this study, due to its ability to create large magnetic flux and further advantages of neodymium iron boron magnets, even for a short stroke length.

In addition to choosing this configuration setup, the generator may still be subject to vibrations, friction and demagnetisation.

Based on Lorentz law, the minimum compression pressure of approximately 5-7 bars may be utilized to produce significant combustion pressure [28], hence the selection for utilization of a 6-bar compression pressure in this study is utilized.
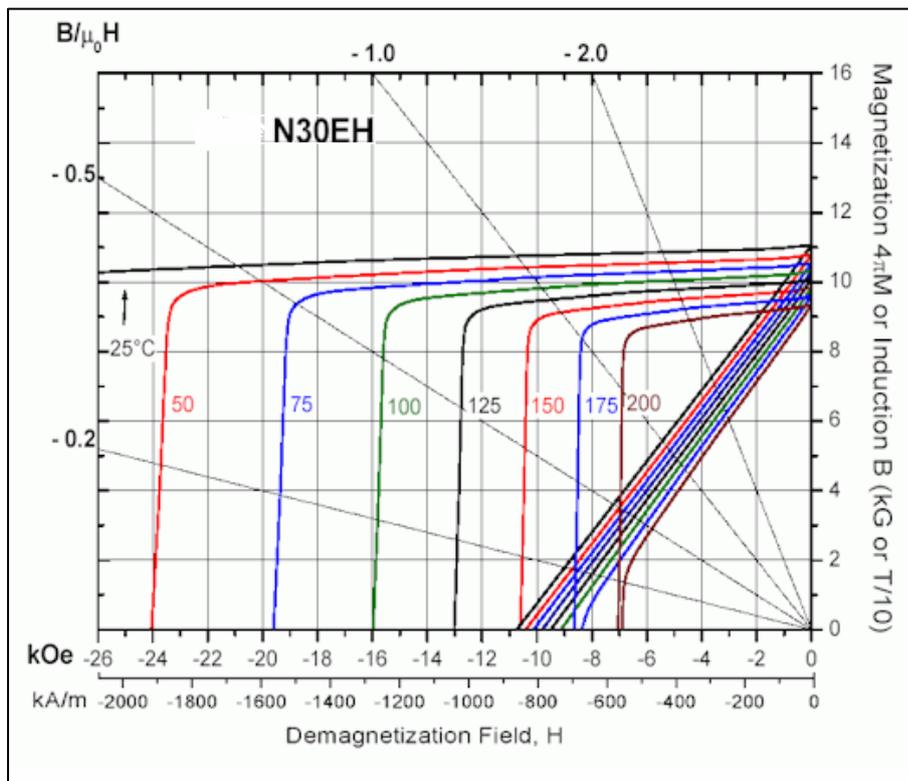
Figure 2.6: Demagnetization curve as a function of temperature for N30EH NdFeB magnet *[27]*

Furthermore, Figure 2.6 demonstrates the importance of coercivity and remanence on the B-H curve as the most critical magnetic properties for permanent magnets (PMs). In addition, B-H curve is used to illustrate the relationship between magnetic flux density and magnetic field strength for a particular material.
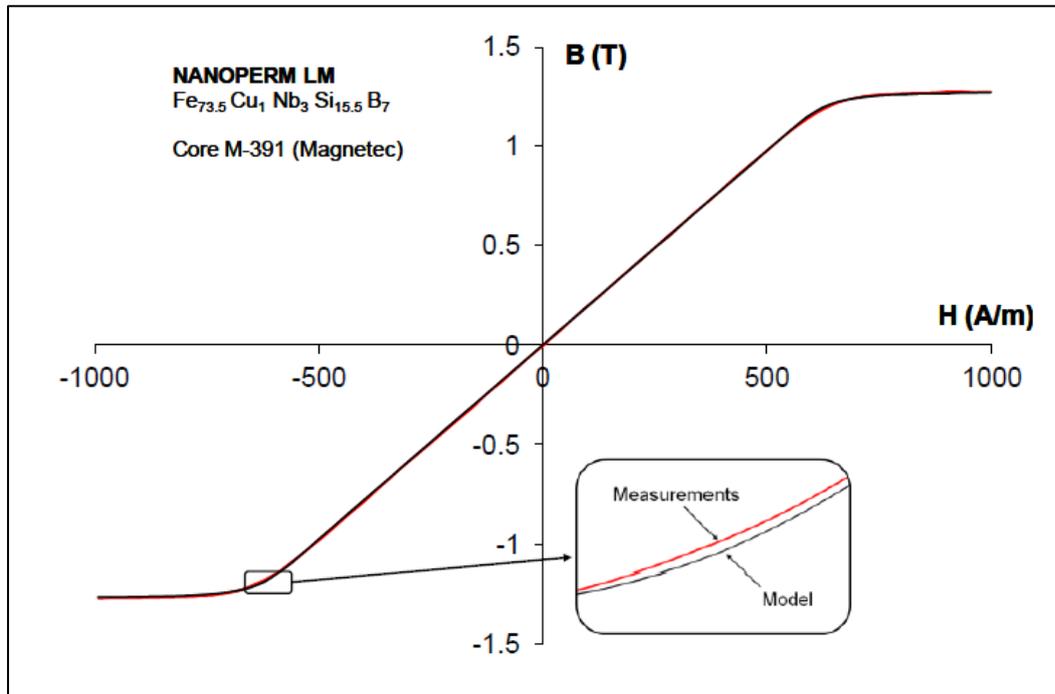
Figure 2.7: example of a B-H curve *[29]*

Neodymium Iron Boron (NdFeB), is selected as the leading candidate magnet utilized for this research. Authors of Ref [30], agree with Mahadi`s observation and further adds that NdFeB magnets may increase flux output in Hci as temperature decreases and is able to change from a uniaxial or easy-axis material to an easy-cone material as illustrated in Figure 2.7.
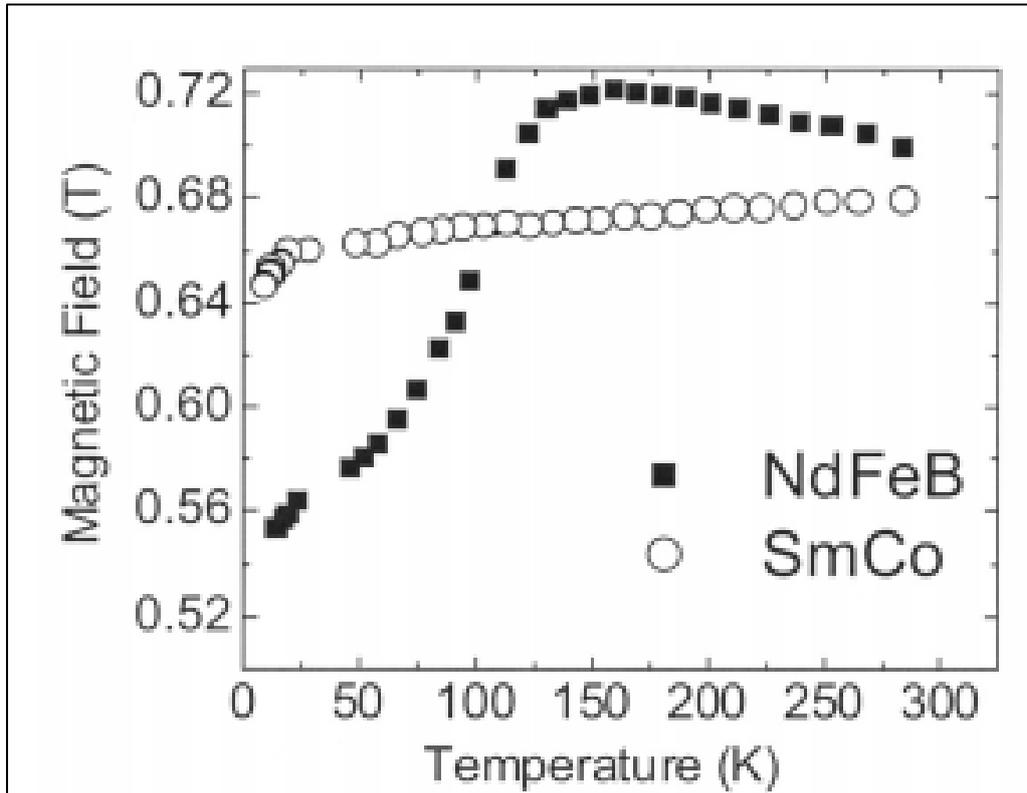
Figure 2.8: Magnetic field as a function of temperature for NdFeB and SmCo *[30]*

The use of NdFeB permanent magnets, over other permanent magnets for this study, is further argued in relation to Ref [31], stating that at room temperature, NdFeB magnets experience strong coercivities $H_{cj} > 24$ kA/cm. NdFeB has a higher energy density than $SmCo_5$ magnets as indicated in Figure 2.8.
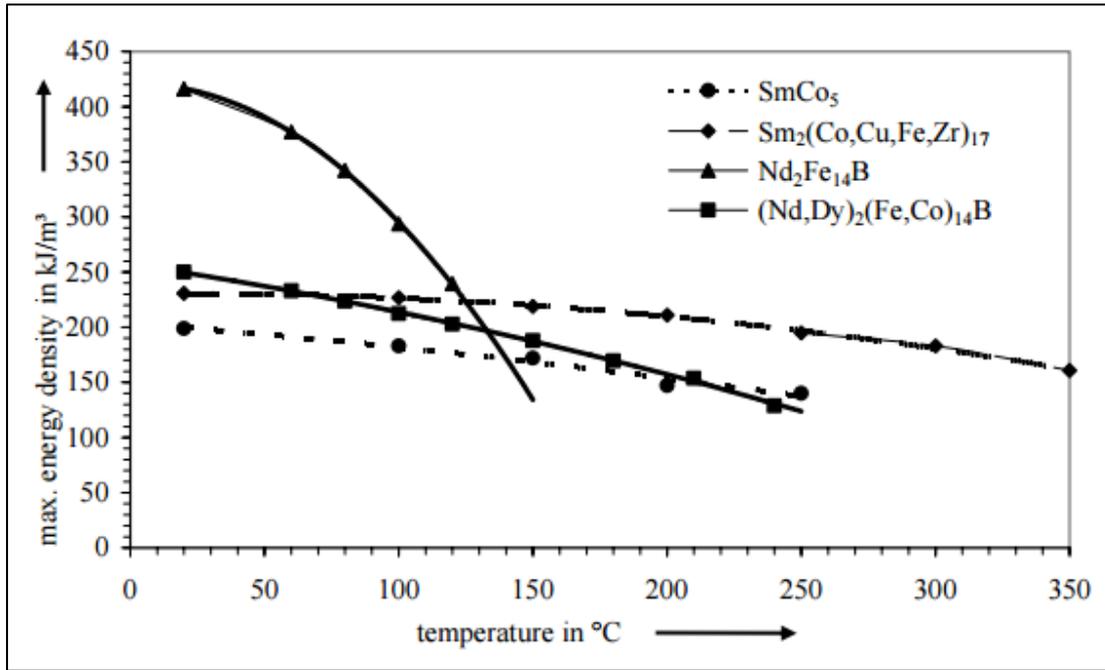
Figure 2.9: Maximum energy density (BH) m of RE magnets in dependence of temperature *[32]*.

Table 2.4 illustrates the magnetic properties of the $Nd_2Fe_{14}B$ magnet as well as the operating temperature range that is equivalent to that of an air piston operating temperature. The following equations demonstrates the necessity of the operating temperature of the magnet as indicated on Table 2.4 and equation 2.16 and 2.17.

Table 2.4: Properties of $Nd_2Fe_{14}B$ magnet

Material Code	Remanence Br				Coercivity Hc				Temp Coeff of Br	Temp Coeff of iHc
	KGs		T		Koe		kA/m			
N35	Typ	Min	Typ	Min	Typ	Min	Typ	Min		
	1.22	1.2	1.22	1.17	11.2	11	891	836	-0.11%/°C (100-20°C)	-0.60%/°C (100-20°C)

$$B_r @80°C = B_{r0} \left(1 + \frac{K_{br}}{100}(T - 20)\right)$$

$$= \underline{1.13948 \text{ T}} \qquad , \qquad (2.16)$$

$$H_c @80°C = H_{co} \left(1 + \frac{K_{Hc}}{100}(T - 20)\right)$$

$$= \underline{0.57024 \text{ MA/m}} \qquad . \qquad (2.17)$$

The linear generator within a free piston engine configuration is assumed to be frictionless and operates under two conditions, *no-load and with-load* condition, as stated earlier in this chapter. The translator motion is kept on by forces generated from the air compressor, resulting in expansion and retraction of air in the engine cylinders, with the control system controlling the entire operation, which will be discussed in detail in Chapter 3.

Cawthorne [33], introduced a force balance engine equation for an engine operating under two conditions; *no-load* and *frictionless*, however, for the study in hand, *the with-load* condition is also accounted for.

The set of conditions as well as the system methodology are applied for conceptual design and development in Chapter 3. However, some of the equations may be modified, depending on the existence and practical complexity of the system.

2.8.   Summary

This chapter has provided an overview of the research developments in the area of power generation. Several papers from utmost referenced journals, conference papers and articles in the area of power generation system control have been reviewed. In these chapter two major points were referenced in relation to literature review; selection of high quality magnets and

power generation strategy. However, only a few research works have been dedicated in both disciples. Literature addressing the use of a free piston engine linear generator as means power generation, the operational strategy, development of a single unit has been discussed. This chapter has also suggested and underlined future works that can make significant contribution to the free piston engine linear generator optimal operation control research area.

Chapter 3: Conceptual, Design and Development of Linear Brushless Permanent Magnet Generator

3.1.   Introduction

This chapter appraises the development and modelling of an FPELG model. Firstly, the physical prototype of the FPELG model and the operational description are provided, as well as the mathematical modelling. However, the cogent proposition of the engine is utilized for progression of the design.

Furthermore, provision for use of geometric combinations for parameters to meet a specific output power of 7W and maximize efficiency with lower mass for the prototype is utilized. The provision is for both the Free Piston Engine physical model and simulation as well as for combustion engines simulation.

3.2.   Linear Alternator Design

The linear engine is an important subsystem and is used as a prime mover of generation system [1]. The engine constructed is tested in two states, the *no-load* state and the *with load* state, with efficiency been tested for both states.

For both states the engine is assumed to be frictionless and engine motion will be kept on by the control systems pushing the pistons inside the linear alternator back and forth, resulting in the action motion of the engine, sustained by the electromagnetism that is experienced in the linear alternator.

The linear alternator consists of two main components, namely the stator and translator. The stator comprises of the exterior of the generator, which is a circular enclosure, with armature winding and back iron. A 3-D cross sectional view of the stator design is illustrated on Figure 3.1.

However, the system development was constructed in (3D CAD Design Software Solid-works) the engine design which was selected as a basis for the development, as indicated on Figure 3.1 to 3.3.

Figure 3.1 presents the measurements for the stator designed, as well as the supporting discs. Figure 3.1 further demonstrates the segment layers of the stator where the coil windings are mounted within each layer, with a supporting lid mounted at the end of the stator to maintain magnetic flux within the stator and to minimize energy losses.

The two scenarios are tested, where a load is connected across the output terminals of the armature windings on the actual generator. As a result, the current flows through the load and power is extracted from the *with-load state,* where the variable resistor is adjusted for both minimum and maximum resistance. Secondly the generator is started and the terminals are mounted on the oscilloscope to obtain the *without-load state.*

The combustion engines assembly is developed in a simulation model with the same objective of designing and developing the same 7 W linear generator.
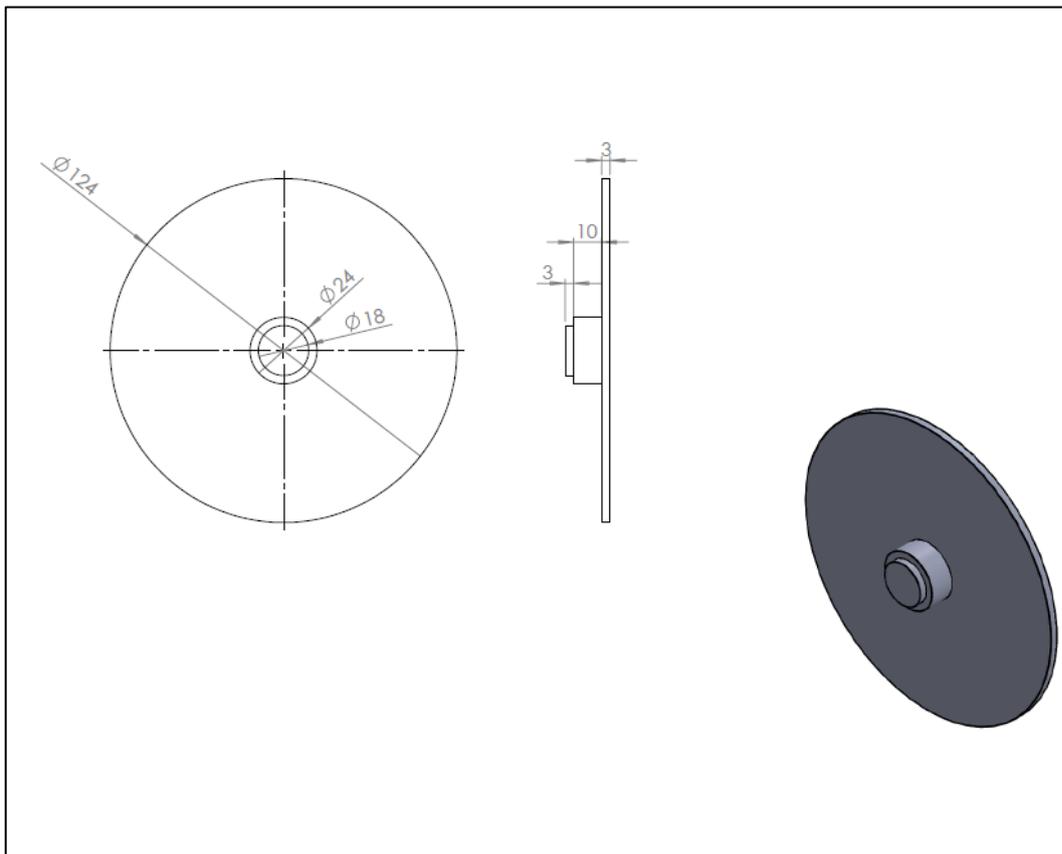
Figure 3.1: Cross-sectional overview stator design

Referring back to Figure 3.1, the lid, or measuring plate, is used as the measuring lid for copper windings across the 10 mm slot, with 3 mm being the closing slot.

However, Figure 3.2 presents the plate used to mount the copper wire where the translator with magnets at expected to pass through during scavenging.

The hole is measured with reference to the magnet and separators circumference, to allow smooth motion of the translator and achievement of high magnetic flux. The windings are turned up to about 90 % of the stator/ plate diameter so that the stator plate can be fitted and the copper wire can join the next plate.

After all seven plates are mounted together, the stator outer lid is mounted with 6 mm nails so as to close the linear generator from Figure 3.3.
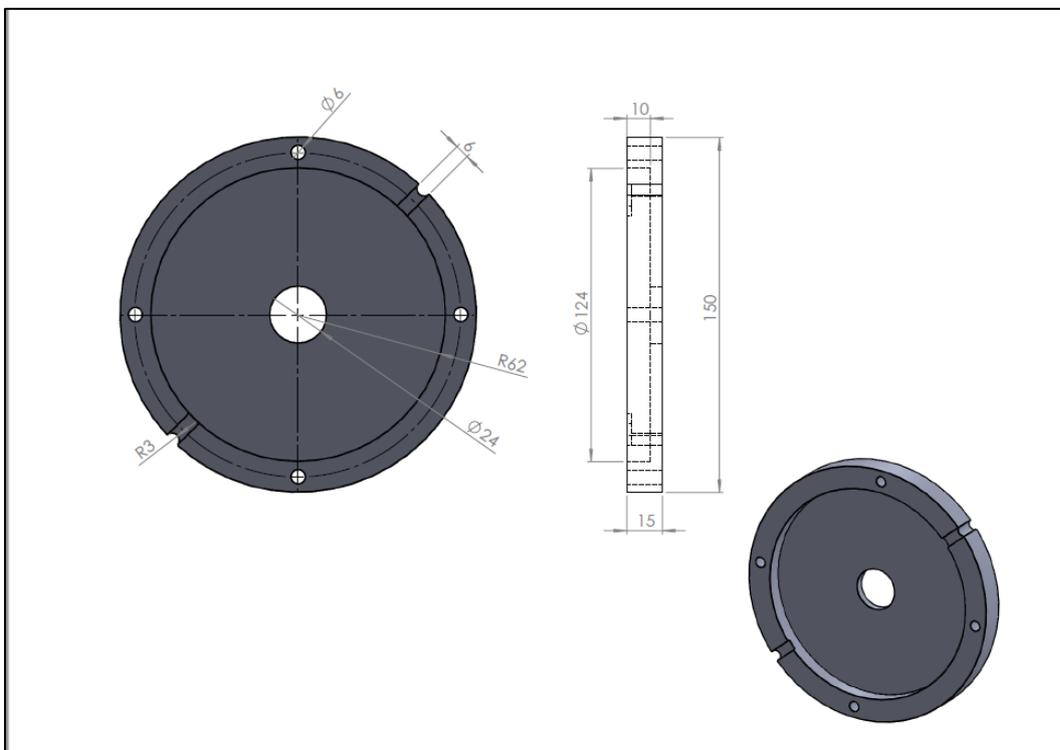
Figure 3.2: Stator plate and cover
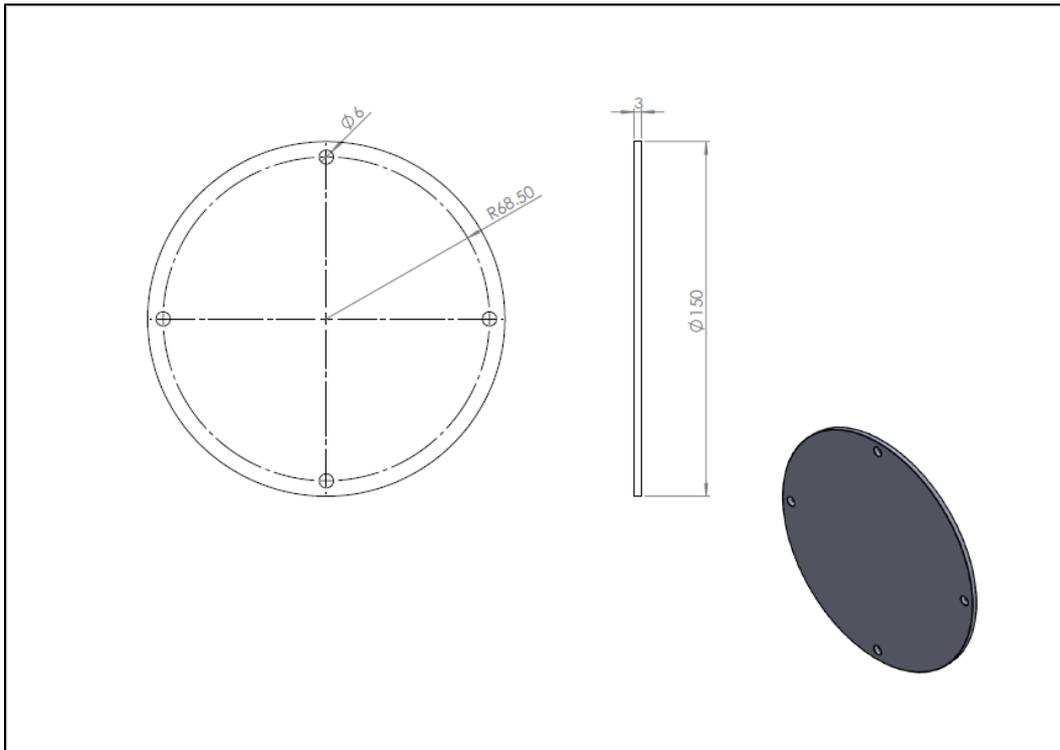
Figure 3.3: Stator outer lid

Figure 3.2 demonstrates the size and shape of stator plate, whereby the coil windings are to be mounted within. For this to take place, seven stator plates are used in reference to the magnets as to experience high efficiency during scavenging. Figure 3.3 demonstrates the specifications of the stator lid that is utilized to close the stator in order to keep the energy intact.

For the stator design, the following attributes are to be considered:

- Minimization of the radial vibration of the stator body
- Allocation space in order to cool the stator down.
- Sufficient space to allow insertion of the coil, as well as smooth scavenging of the translator mounted with permanent magnets.

The engine comprises of two pistons on each side (dual piston), which is free to oscillate within the cylinders shaped bodies of the engine as indicated in Figure 3.4.

29
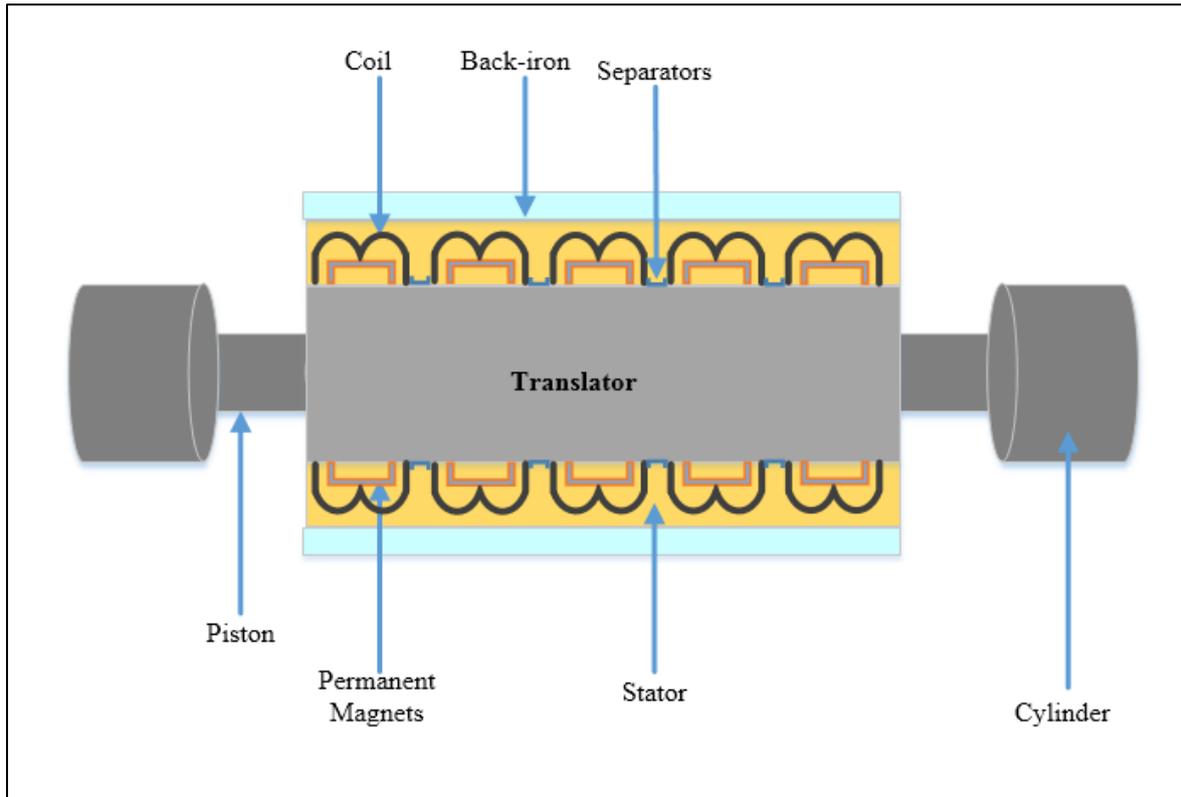
Figure 3.4: Cross sectional view of linear engine with linear alternator

For the study presented, combustion occurs at each end of the generator, rather than inside the alternator, whereby the cylinder head fully extends to the opposite end, however, with the hall-effect sensors preventing collision of the cylinder heads with the stator.

The importance of permanent magnets in energy generation is expressed in Faraday`s law, which relates to the rate of change in magnetic flux, through a loop to the magnitude stating that:

$$e_{induced} = -\frac{d\emptyset}{dt} \qquad (3.1)$$

Where:

$e_{induced}$ = induced voltage on the coil

$\emptyset$ = flux in the coil

However, the equation (3.1) can still be modified and applied with reference to Lenz`s law as follows:

30

$$e_{induced} = -N\frac{d\emptyset}{dt} \tag{3.2}$$

Where:

$\emptyset$ = flux passing through one coil per turn

N = number of turns in the coil

The permanent magnets are mounted onto the translator to create a magnetic field during scavenging inside the coil windings of which are mounted directly on the stator. A translator is moved through the stationary coil windings that are mounted directly on the stator surface. As a result, the voltage will be induced referring to Faraday`s Law.

The generator design was accomplished by removing the crankshaft mechanism and replacing it with a translator. The stator was developed in such a way that it can accommodate ~300 coil windings, without being exposed to the magnets with reference to American Wire Gauge (AWG), named on Table 2.3 and to meet the 90 % proximity of the stator plate. Furthermore, in order to accomplish the motion, several factors such as frequency and control systems had to be considered first.

However, they will be discussed at a later stage as well as their applications to the generator operation.

3.3.   Combustion Engine Design

The combustion engines are engines of which piston motion is controlled by means of crankshaft mechanism for energy generation. Crank is defined as an arm attached at a right angle to a rotating shaft, of which the reciprocating motion is imparted or received from the shaft [34].

Since generators operate on the same principle, the Free Piston Engine, as well as the crankshaft engine, have the same process occurrences inside the cylinder [35], [36]. However, their motion sequence is different. For the slider-crank mechanism, the following model is subject for external forces as indicated in Figure 3.5 below.

For the present study, a flywheel is utilized due to its advantage to rotate at 360°, while attached to a stand-alone pole. The kinematics are mostly based on the flywheel motion. However, several authors measure kinematics on an angular based relation, which is not accounted for in this study, hence the use of the flywheel for the mathematical model.
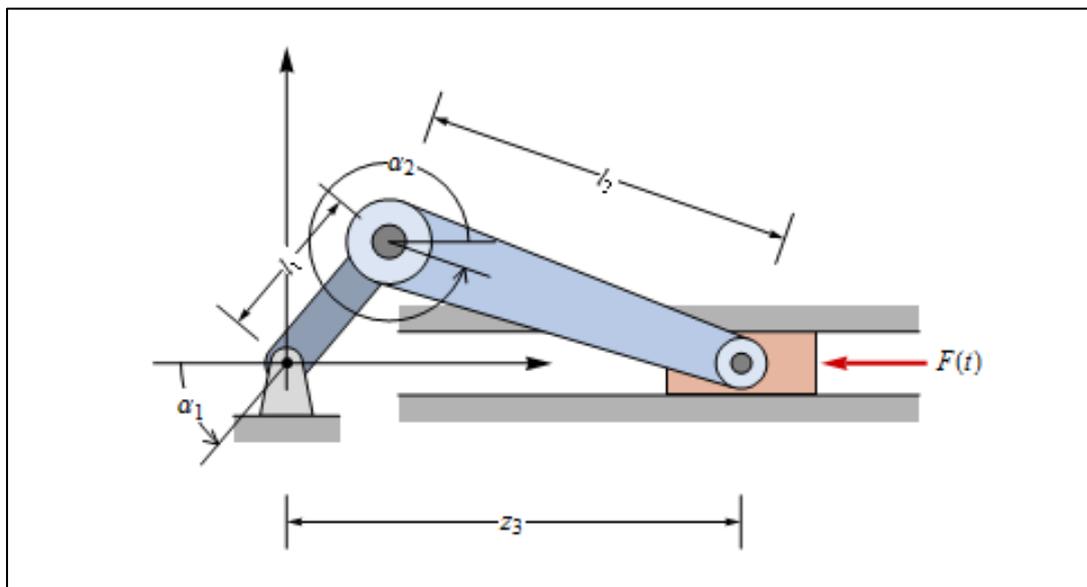
Figure 3.5: Slider crank mechanism *[37]*

Figure 3.5 highlights the angles, as well as the total frictional losses that occur on a rotatory engine. However, authors of Ref [36], highlights valves, pistons and piston rings as the major contributing factors for frictional loss in a combustion engine [38].

32

Due to technological improvements, different piston designs are utilized in order to reduce friction on the engine.

Figure 3.6 demonstrates the forces that are acting on the piston. Evidently, reduction of the weight and skirt of the piston also reduces the frictional losses on the engine.
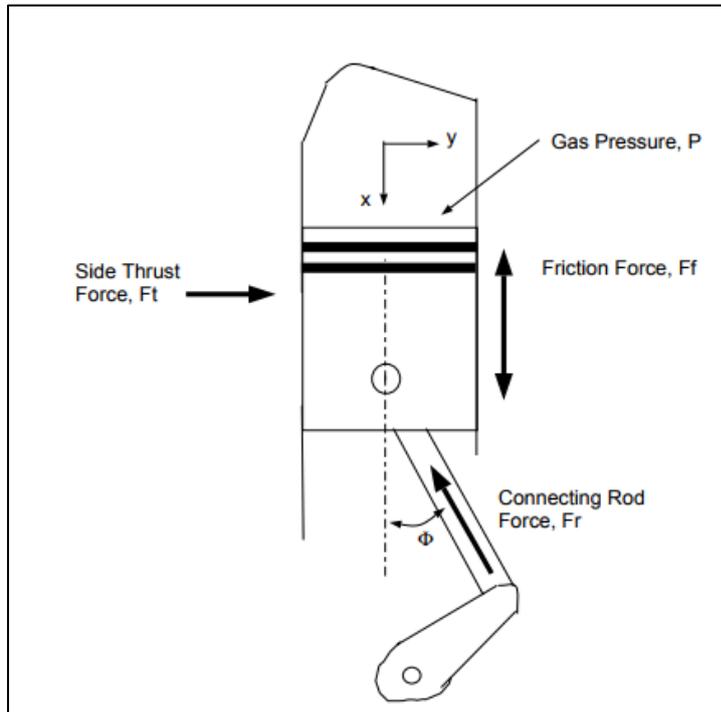
Figure 3.6: Forces acting on a Piston *[38]*

3.4. Methodology for Simulation and Starting of FPELG

The operation in starting the engine depends on several fundamentals, namely the air pressure and the electrical power supply that is used to power the control system.

Since the methodology for starting FPELG depends not only on the control systems, but the mechanical forces acting on both pistons are also accounted for. This process of starting a FPELG comprises of the following fundamental steps:

- Air pressure is supplied from the air compressor to the intake valves of the system. However, the motion direction is needed, and it is therefore accomplished by supplying the air pressure to the air switch instead of the intake valve.
- The air switch is directly connected to the control systems, which control the piston motion speed, motion direction and cycle duration.

The control systems development and functionality will be highlighted in depth in section 3.6.

The initial motoring speed for starting the engine is initiated by both the 6 bars air compressor and the control system. However, since there are several energy conversions during Free Piston Engine Linear Generator operation, kinetic energy is assumed to occur at the start of the operation where it is determined as follows:

$$K_e(during\ start) = \frac{1}{2}mv^2, \qquad\qquad (3.3)$$

$$= (\frac{1}{2} * ((3.64) * (0.25)^2),$$

$$= \underline{\textbf{0.11 Joule}}.$$

K_e represents Kinetic energy, m represents the load mass and v represents the velocity.

However, for the measurements utilized in equation 3.3, m is obtained from 3.15 of sub-section 3.3 and v is the velocity obtained from Chapter 4 in section 4.1 of the results.

After obtaining the energy needed to start the engine motion, the theoretical output power should to be calculated in order to identify whether the model can achieve the proposed objective or not.

Therefore, power is calculated as follows from the kinetic energy obtained in equation 3.3 as follows:

$$P_n = \frac{Energy}{Duration\ per\ Stroke},$$ (3.4)

$$= \frac{0.11}{0.02},$$

$$= \underline{\mathbf{5.5\ W}}.$$

Where P_n = Power,

The stroke used in equation 3.4 is obtained from the stroke length of the system which is 100mm which is identified in Table 4.1 in Chapter 4.

The piston motion is important in achieving electromagnetism, since the efficiency of the system depends on it. Therefore, dynamic equation as well as piston motion are simulated and implemented on Matlab$^@$/Simulink and a physical prototype is constructed for verification of results. Furthermore, piston motion for this study was achieved by deriving Newton`s second law, stating that:

$$F_m + F_l - F_r - F_f = m\frac{d^2x}{dt^2}$$ (3.5)

Where:

F_m = Magnet Force ,

F_l = Force from the left cylinder,

F_r = Force from the right cylinder,

F_f = Frictional Force .

However, Equation 3.5 can further be simplified into Equation 3.6. Since frictional force is not accounted for in this research and is treated as a constant due to the reasons stated above, resulting in Equation 3.5 being modified and re-written as Equation 3.6 as follows:

$$F_m + F_l - F_r = m\frac{d^2x}{dt^2}$$ (3.6)

The modelling of the engine is designed as to reduce frictional losses as low as possible, therefore the concept of shaft stabilization was used for the achievement of high efficiency

35

for the working of FPELG. It is significant, since the aim is to accomplish piston stability in the design due to its vital role in frictional loss reduction, as indicated in Equation 3.6.

The magnet setup as indicated in Figure 3.7, with the translator passing in the middle of the alternator, demonstrates the stability and piston synchronization. However, the translator stability (based on load mass) calculation is provided at the later stages of this section providing a clear picture whether the translator can withhold the magnets and separator mass.

In addition to Equation 3.6, a dynamic balance equation of motion is utilized, since the translator motion converts the chemical energy through combustion chambers, into kinetic energy of the moving mass, into electrical energy through the generator.

The mathematical formulation is used as follows as to simplify the dynamic modelling of the system, by applying Newton`s second law of motion as follows:

$$\sum F = F_{mot} + F_p - F_f - F_{cog} = m\ddot{x} \qquad (3.7)$$

Where: $\sum F$ = total force,

F_{mot} = Motor force,

F_p = In-cylinder pressure force,

m = moving mass,

$\ddot{x}$ = piston acceleration.

Figure 3.7, demonstrates the assembly of both magnets and separators on the translator. However, Figure 3.7 highlights the stability (mass) to optimize the translator.

Figure 3.7: Side view of the Engine showing magnets and separators

Figure 3.7 Side view consists of the structural arrangement that is used for the cylindrical linear generator. The arrangement consists of (1) magnet and (2) magnetic separator to keep

magnets away from each other to illuminate magnetic attraction. This arrangement consists of seven permanent magnets and seven magnet separators (non-magnetic objects).

The arrangement outlined in Figure 3.7, determines the velocity of the system which is based on two aspects namely the translator length and two connecting pistons to the translator. The following equations are derived in order to obtain the system velocity using an input air pressure of ~6 bars:

$$\sum PT_L = P_L + P_R + T_L \qquad (3.8)$$

Where PT_L = Piston_Translator Length,

P_L is the Left Piston,

P_R is the Right Piston,

T_L is the Translator Length.

As a result, the sum of the entire movable object contributes to the system length. The FPELG velocity derived from Equation 3.1 is based on a load-less translator:

$$v_s = \frac{D_s}{t_s} \qquad (3.9)$$

Where v_s = System velocity,

D_s = System Displacement,

t_s = System duration.

However, the load-less translator does not contribute to any energy generation, since magnetic flux is not present due the absence of magnets. The usable velocity with total load mass is indicated in Figure 3.8. As a result, Equation 3.10 can be derived from Figure 3.8 as well as modification of Equation 3.8.

$$T_L = \frac{\Delta V_s}{L_m} \qquad (3.10)$$

Where: T_L = Translator Load,

Δv_s = Change in velocity,

L_m = Load.

The load mass (L_m) is obtained from Equation 3.15, where both the magnetic mass and separator mass are compared against the translator mass.
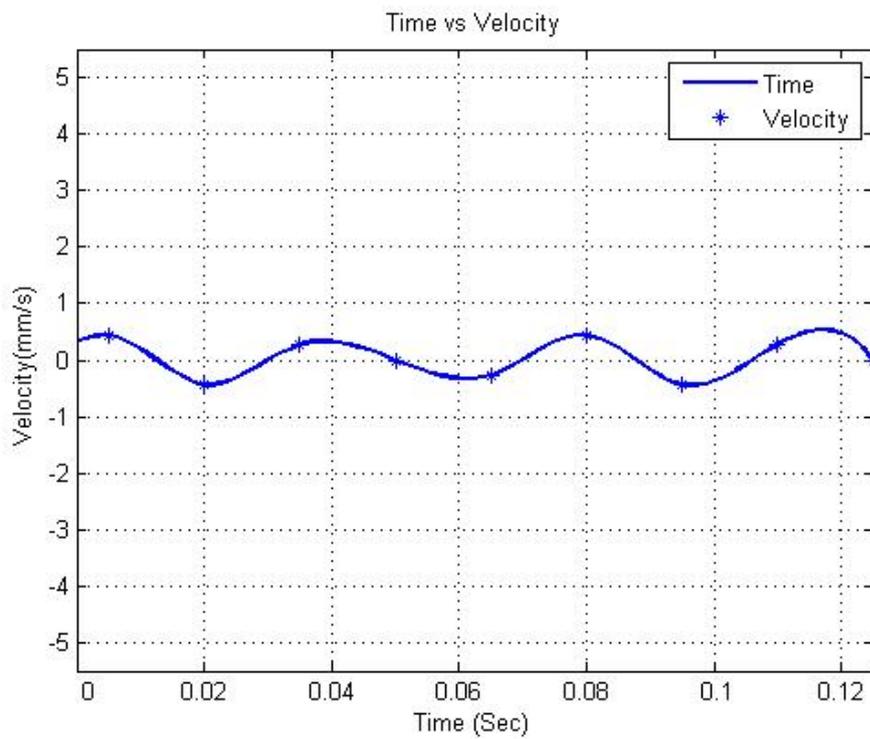
Figure 3.8: Velocity with max load for energy generation

The output voltage depends on the velocity of the system. Due to this factor, velocity is assumed to be the determining factor of the output voltage, as the air pressure is kept at a constant pressure of 6 bars, with the control system sustaining the air direction and speed.

38
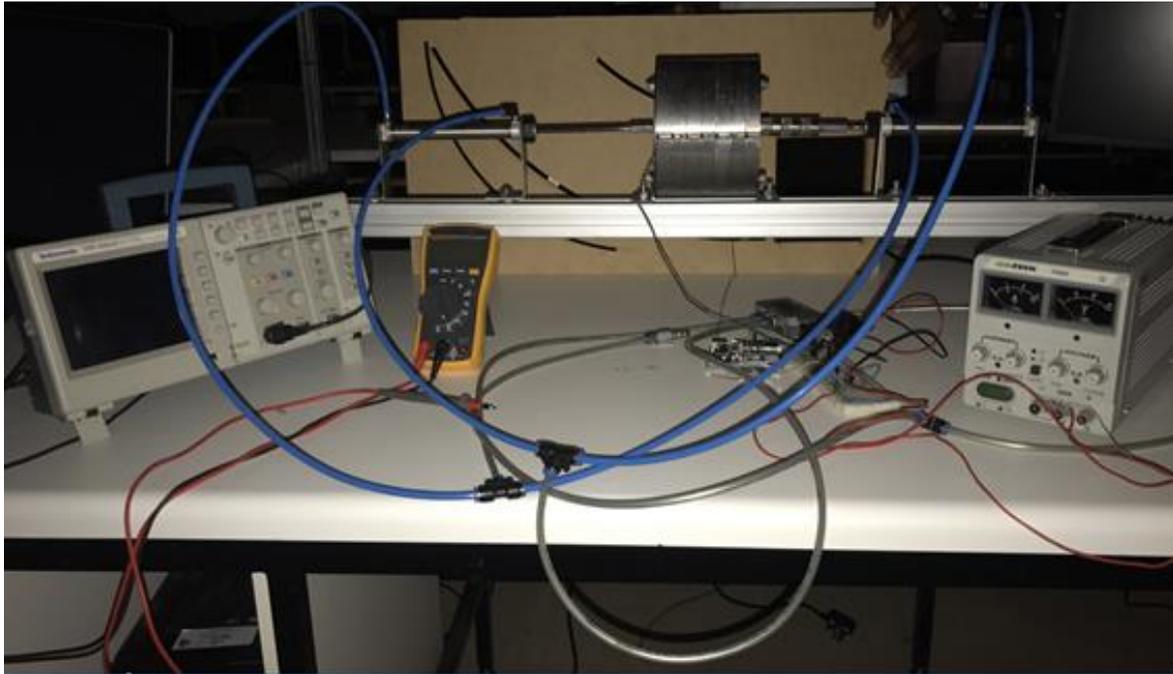
Figure 3.9: FPELG Prototype

A linear generator was integrated in the middle of the engine, with combustion chambers at both ends as indicated in Figure 3.9. The linear machine is operated as a linear generator during the process of energy generation, as indicated in Figure 3.9.

Furthermore, the piston motion is achieved by applying air pressure onto the air switch, which will allow for air pressure to pass to either the left or right cylinder for extraction and retraction. The dual FPELG build can maximize or minimize the output power, while a compact design can be realised by utilizing both combustion chambers, acting as rebound devices during scavenging.

The control system enables the pistons to move back and forth to produce energy within the generator. The linear generator is operated in a closed loop. However, since combustion happens at each end of the generator, the air inside the cylinder compresses and expands as the piston moves into and out of the cylinder, absorbing and dissipating energy respectively.

As a result, the ideal gases for both compression and expansion processes are administered by the same relationship between pressure and volume inside the cylinder [39].

$$P_1 V^k_1 = P_2 V^k_2 \qquad (3.11)$$

39
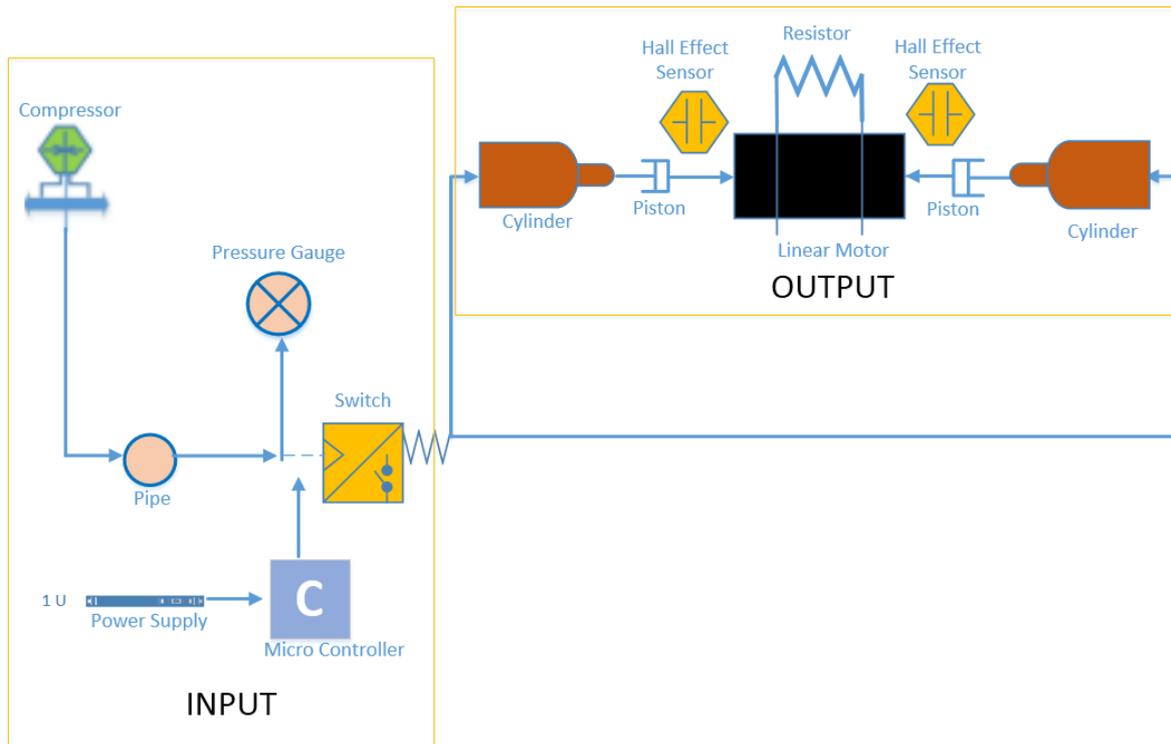
Figure 3.10: Proposed Dual free piston engine linear generator configuration with control system with a resistor

Figure 3.10 highlights the entire generator setup, where the system consists of both the input and the output segments, which are for the *with-load* scenario, due to the load resistor. However, the linear generator equivalent circuit is outlined at a later stage, to view the components used in modelling the generator.

The system input and output are derived from equation 3.11 and 3.16, which is derived as follows:

$$S_s = P_{LR}V^k{}_{LR} + V_{in} - Ri - L\frac{di}{dt} \qquad\qquad (3.12)$$

Where:

Ss = System Setup,

S$_I$ = System Input,

S$_o$ = System Output.

Which are in reference to Figure 3.7, whereby the engine is divided into two parts namely;

Systems Input (S$_I$) and System Output (S$_o$).

Figure 3.7 further demonstrates the translator mass, which is the sum of piston mass, separator mass and magnet mass.

$$T_{mass} = P_{mass} + M_{mass} + S_{mass} \qquad (3.13)$$

Since the sum mass of the piston, magnets and separators surpass translator mass, this results in a bend of the translator eventualizing in frictional losses during scavenging, as the translator strike the stator during scavenging.

$T_{mass} \propto Sum_{mass}$ Translator mass is indirectly proportional to the sum mass (piston mass, magnetic mass and separator mass)). However, for the purpose of this study frictional losses and other kinds of unknown energy consumptions are ignored, except the bearing frictional losses in the simulation.

$$M_{mass} = T_{mass} - P_{mass} - S_{mass} \qquad (3.14)$$

Where:

T_{mass} is the Translator Mass

P_{mass} is the Piston Mass

M_{mass} is the Magnetic Mass

S_{mass} is the Shaft Mass

Furthermore, in relation to mass effect on the system, the force balance equation plays an important role to reduce frictional losses between the magnet thrust and stator core of the generator. However, for this study balance equation is ignored but rather the magnetic mass as well as the separator mass acting on the translator, are shown, but not their effect towards the efficiency of the system.

The total load mass can be obtained using the following equation:

$$L_m = ((M_m * N_m) + (S_m * N_s)), \qquad (3.15)$$

$$= (0.0214 \, kg * 7) + (0.5g*7) \, [40],$$

$$= \textbf{\underline{3.64 kg @ 4.7kg pull force.}}$$

41

Authors of Ref [39], highlights the magnetic mass which is obtained from the manufacturer`s datasheet. However, the separator mass is based on a combined Perspex mass, which is ~0.5g with the same diameter as the magnets used.

The design configuration as indicated in Figure 3.7, presents the generator arrangement comprising of seven magnets and seven separators:

Where L_m denotes Total Magnetic mass

M_m is the Magnetic mass,

N_m is the Number of magnets,

N_s is the Number of separators,

S_m is the Separator mass.

As a result of the heavy magnets attached on the translator, the piston velocity reduces and impacts the voltage-producing capability of the system, as stated in Figure 4.1 in chapter 4.

3.5. Linear Electric Alternator Model during Steady operation

Section 3.2 outlined the methodology for starting FPELG, as well as the alternator modelling. However, since the main objective of this research is concerned with the output power as well efficiency of the alternator, it is important to examine the electrical model of linear alternator.

The linear generator operates as a generator during a steady operation. The translator forms part of the piston moving assembly as it is directly mounted to both pistons in the system through scavenging process [41]. However, this results in electric current being generated from alternator coils.

The linear generator operation is usually periodic during motion of the FPELG and the velocity of the two pistons fluctuates between zero and maximum in both negative and positive directions. As a result, the system is sustained by the electromagnetism and is a stand-alone system. In addition, Figure 3.11 illustrates the electrical equivalent circuit of the alternator as a single phase.
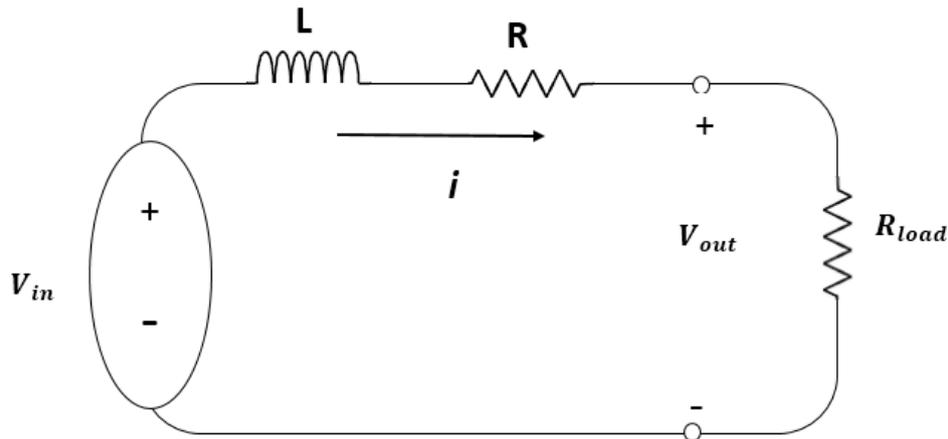
Figure 3.11: Single phase equivalent circuit for linear alternator

The voltage equation for Figure 3.11 can be denoted as

$$V_{out} = V_{in} - Ri - L\frac{di}{dt} \qquad (3.16)$$

[33]

Based on literature, different authors agree on the use of 100 mm stroke length, at a considerable frequency of 10 Hz – 40Hz, were reported to be good for FPE prototypes in a *no-load state/ condition [42]*. However, for this research, 100 mm stroke length, as well as 40 Hz frequency is used for both *with-load* and *without-load* state, based on the literature. Since the research is aimed at evaluating efficiency of a linear alternator at a specified frequency range, the ultimate goal is reaching 60 Hz.

An Average piston force of 112.5N@6bars is used for extraction and retraction. It can also be determined based on the efficiency, rated power, as well as average linear speed, ignoring the mechanical losses. Furthermore, the electric machine can be used as a generator, both for starting and stopping the translator motion and also as a generator for energy conversion, as indicated in Figure 3.11. Since there is an absence of crankshaft mechanism, the translator is not restricted, therefore, compression ratio can be experienced *[43]*.

3.6. Development of Crankshaft Simulation

The slider crank mechanism may be defined as the mechanical tool used for conversion of straight motion to rotary motion as in reciprocating piston engine. Figure 3.12 below

43

highlights the simulated frictional losses results, based on a crankshaft mechanism, which are presented in Chapter 4.

The methodology of developing crankshaft simulation is based on Figure 3.12.

The three major components: piston, connecting rod and crank, are determining factors of both the frictional and power losses that occur at an angular Ø, where either the connecting rod or the crank controls the motion. However, for this study, both the crank and the connecting rod are used as non-stationary objects that conduct motion simultaneously.

The Ø is an important parameter, due to the fact that during motion, the angle of the generator will be changed for the entire cycle since a flywheel is used. However, the angular velocity, acceleration and other related mechanisms are not accounted for.
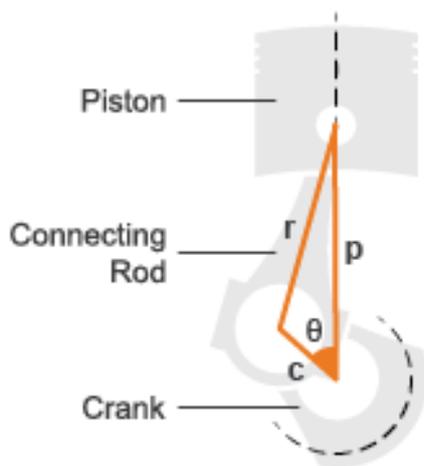
Figure 3.12: Crankshaft mechanism diagram *[44]*

The following equation explains the relationships between the friction formula as well as the cylinders involved. However, due to the changing angle degree during operation, an idealized angular degree is used in accordance to the crankshaft losses. The design is also based on the air pressure supplied, as well as the crank bearings, which are not highlighted in Figure 3.12.

An angular degree of $45°$ to $180°$ is used relative to Figure 3.12, where crank motion is only account for in the simulation design code. Both sub-section 3.2 and 3.5 are focused on the development of combustion engines. However, sub-section 3.5 is focused mainly on the methodology for calculating the losses during the operation.

The angular frictional losses are not accounted for, i.e. the methodology used here does not account frictional losses at a particular angle, but rather the overall frictional losses during generation operation.

$$d = C_n * b^2 * L_s \qquad (3.17)$$

Where: d is the denom,

Cn is the number of cylinders,

b is the bore hole,

Ls is the stroke length.

$$F_b = (C_b * S_b * N^{(0.6)} * D^3{}_b * B_L)/d \qquad (3.18)$$

Where:

Fb is the Friction of crankshaft,

Cb is the Crankshaft bearing,

N is the engine speed,

Db is the bearing diameter,

Bl is the Bearing length.

$$F_C = (S_c * D_b)/d \qquad (3.19)$$

Where:

Fc is the frictional loss on the crankshaft,

Sc is the crankshaft seals.

45

3.7. Development of a Control System and Air Piston Dynamics

The research is concentrates on the generator efficiency and not the development of the piston engine. A replacement was necessary for the simulation of the free piston engine scenario thus the inclusion of the air piston dynamics integrated with cylinders as in Figure 3.13 below.
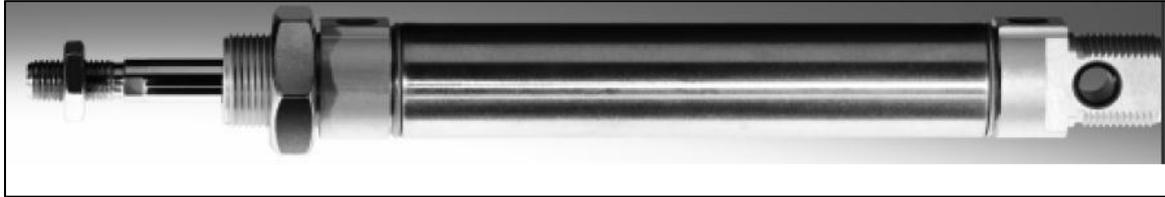
Figure 3.13: Air pistons with cylinder integration

The piston assembly, showed on the Figure 3.13 above, illustrates the air piston with each segment namely: the piston rod end, bounce piston end, piston stroke length and the cylinder.

However, since the air piston dynamics of the FPE designed comprises of such units, an equation can be denoted by using the following equation:

$$\ddot{x} = \frac{1}{P_m}(F_{Piston_{left}}(x,\dot{x}) - F_{Piston_{right}}(x,\dot{x}) - F_f(\dot{x}) + F_{linear_{alternator}}(x,\dot{x})) \quad (3.20)$$

Where: Pm is the piston mass,

$F_{pistonleft}$ is the Force from the left piston,

$F_{pistonright}$ is the Force from the right piston,

$F_{linearmotor}$ is the Force from the linear alternator,

F_f is the Frictional Force.

Equation 3.20 may, however, be simplified further to Equation 3.21 in order to relate to Figure 3.14, with the assumption that frictional force is zero for the purpose of the research:

$$\ddot{x} = \frac{1}{P_m}(F_{Piston_{left}}(x,\dot{x}) - F_{Piston_{right}}(x,\dot{x}) + F_{linear_{alternator}}(x,\dot{x})) \quad (3.21)$$
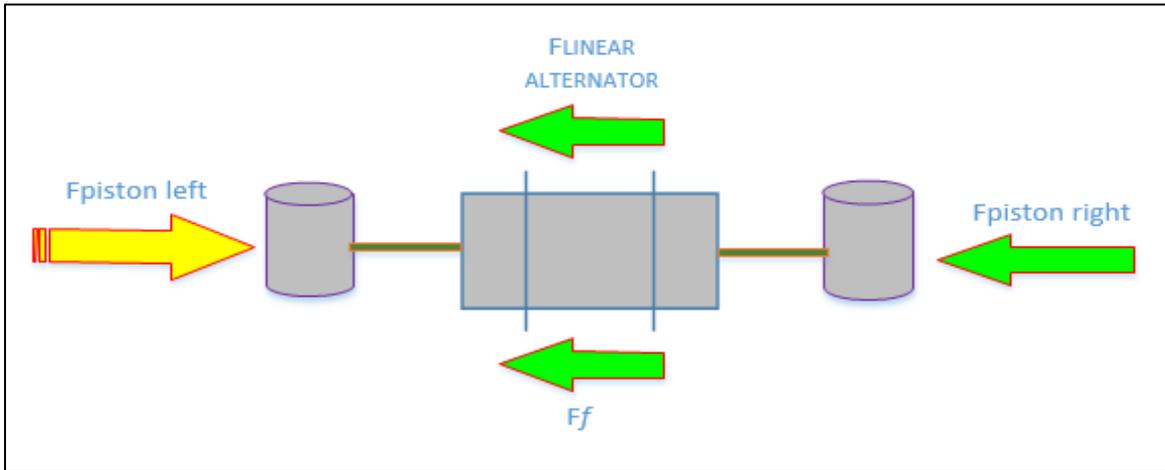
Figure 3.14: FPELG with forces acting on it

During the component selection, parameters identification are ideal and important phenomena, since they provide a guideline of what will be obtained as the final product.

Table 3.1 illustrates the parameters of the selected air pistons to be used for this research, importantly their ability to function at an operating temperature similar to the magnets operating temperature, as illustrated in equation 2.15 and 2.16.

Table 3.1: Main parameters of piston with cylinder

	Stroke Length	Average Weight	Average Force	Average Speed	Operating Temperature
Units	mm	g	N	mm/s	ºC
Measurements	10…100	47,25	112,5@6bar	2,95	+5 - +80

Figure 3.15 illustrates the control systems used in this research and the components used are outlined.

47
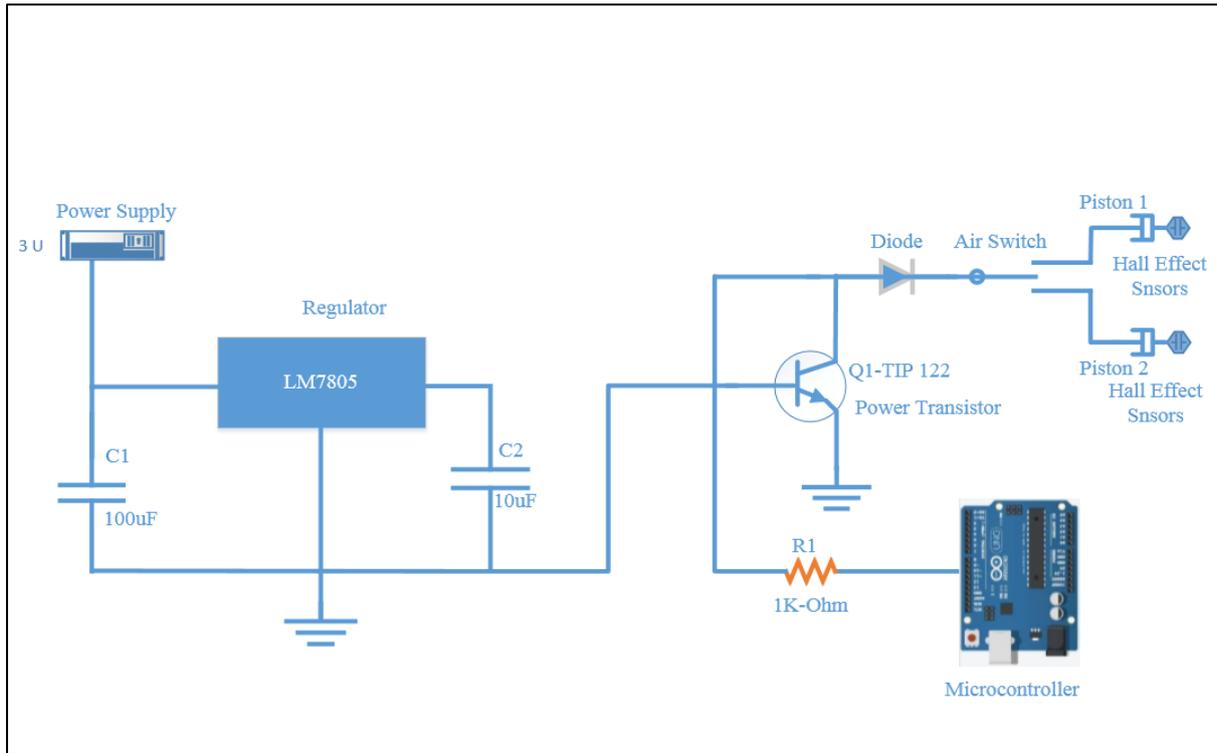
Figure 3.15: Control System physical setup

The control system illustrated in Figure 3.15 consists of the following components:

- Microcontroller
- Air Switch
- Power transistor
- Regulator
- Hall effect sensors

Figure 3.15 provides a view of the control system. The control system is designed to control the movement of the generator, as well as to obtain the generated power feedback from the feedback circuit to the oscilloscope or multimeter.

In the control system, the microcontroller acts as the brain of the system, instructing the air-switch on the time and direction in which the piston moves. A 24 VDC power supply that is used to power the system is therefore regulated by a 5 VDC regulator to prevent the microcontroller from burning.

The regulator is used to regulate the voltage from the power supply to allow the microcontroller to function at an acceptable input voltage of less than 7 VDC. The air-switch is operated through the power transistor.

48

Furthermore, piston dynamics and control for this research are controlled by the microcontroller. Figure 3.16 illustrates the properties of FPELG control structure and highlights the sequence of the FPELG operation. Due to high level of motion, throttling occurs per cycle as the load increases and the compressor cuts the air supply with a direct command from the control system.

In this research, hall-effect sensors were used to determine at what time the magnets are close the cylinder and the pistons have fully extracted or retracted. A switch was used for interface with the microcontroller for feedback and motion control of the air pressure from the air compressor to the engine.
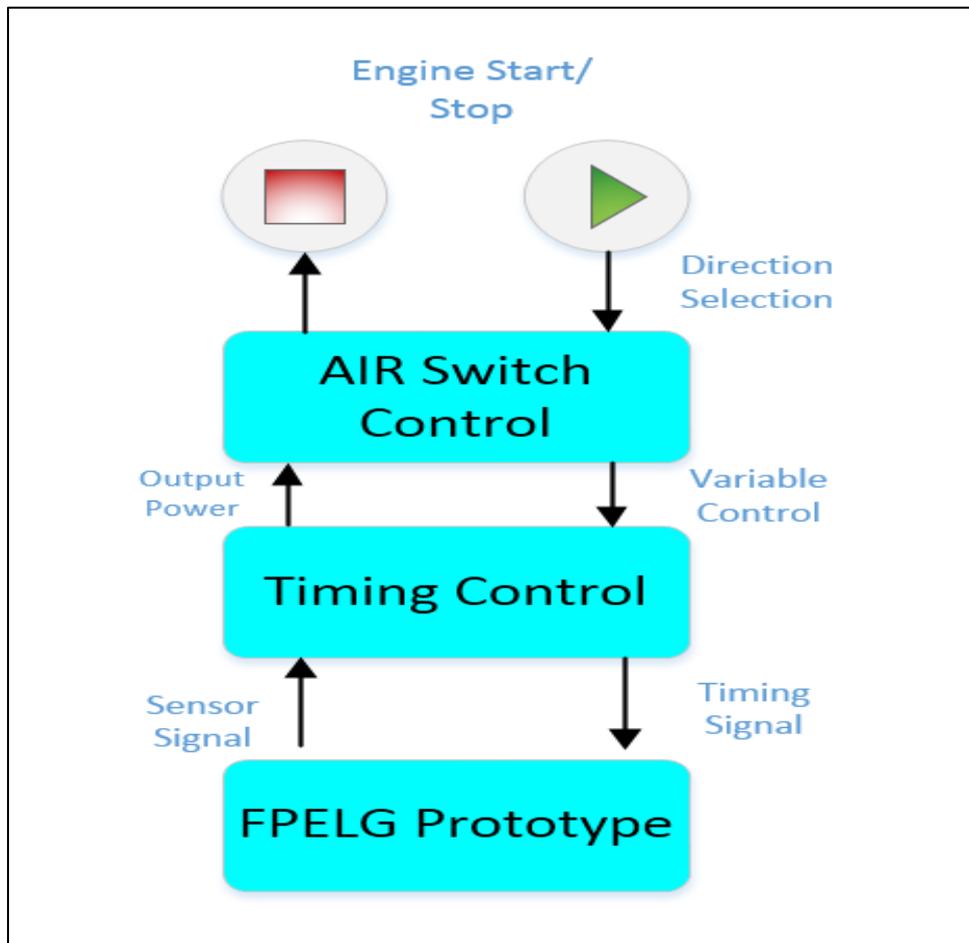
Figure 3.16: FPELG control Structure

Figure 3.16 highlights the control structure sequence of the generator. Before the engine is started, the control system acts as the brain of the engine. The engine is pre-programmed to operate for three cycles. The air switch therefore controls the air direction from the air pressure, as well as extraction or retraction of piston motion.

49

Thereafter, the timing control system controls the cycle duration and transmits the signal to the linear generator; as a result, scavenging occurs and the mechanical energy is converted to electrical energy.

The outcome of energy conversion during scavenging, is the electrical model and control system determines the system efficiency. However, Chapter 4, elaborates the results obtained during execution and testing of the methodology, explained in Chapter 3. The methodology provides techniques to measure current, velocity, voltage and power.

3.8.   Summary

In this chapter two mathematical models have been developed for both free piston engine linear generator and combustion engine. The problem objective function for developing a physical model with the same specifications as used in the mathematical model has been developed. However, the accuracy which is time based for the control system in firing pistons has also been developed bearing in mind the magnets and separator weights that surpluses the translator weight and results in bend of which leads to frictional losses occurring in FPELG. The performance of the generator can be analysed based on both the control system and power generated.

Chapter 4: Simulation and Results

4.1. Introduction

This chapter examines the results obtained from the simulation model developed and built system. The results are presented and evaluated to prove a concept of a linear generator power generator model as a physical and simulation model. The results presented here, demonstrate various simulations and variable testing methodologies for two test case scenarios (*with-load and without-load*).

The design of the system contributes to losses that take place within the generator configuration setup (bearing), however, it has been indicated that the study doesn't focus on losses such as frictional, mechanical and heat dissipation apart from copper losses, which are accounted for only in the simulation results. Losses experienced during scavenging are lower in the simulations compared to the physical model, including the system efficiency. The results provided in this chapter are based on a generation frequency of 40 Hz due to the practical setup.

According to evidence provided in this chapter, the linear generator is more efficient as compared to combustion engine. The finite distinction between the generators is due to the difference in mechanisms. It has been proven according to Figure 4.3 which resembles a simulated free piston engine linear generator output power is closer to the anticipated output power as per hypothesis and study objectives suggested.

Furthermore, it can be argued that the combustion engine does have higher frictional losses, yet produce approximately the same output power. However, this argument has been answered based on both literature and the results presented. Due to higher frictional losses experienced in a combustion engine operation as presented in Figure 4.9, the energy losses also increase, which therefore results in lower power ratio, as a result number of turns had to be increased in order to compensate for losses of which it makes benchmarking impossible since components are not the same.

4.2. Linear Generator Simulation Preparation

The simulation is performed on two model configurations: Matlab[@]/Simulink and the physical model. The objective of the research is based on the output system efficiency. From the physical model, the output voltage was obtained and converted to power using ohms law and the efficiency of the system presented. Table 4.1 demonstrates the achieved results of the system built, using parameters highlighted in the study.

The reciprocating movement of the translator within the linear generator produces pulsing alternative current (AC), as illustrated in Figure 4.2.

Table 4.1: Linear Generator specifications

Variables	Units
Output Power	7 W
Frequency	40 Hz
Air Pressure	6 bars
Force	112,5 N
Velocity	24 mm/s
Magnet Mass	3,64 kg
No of Magnets	7
No of Separators	7

Referring to Table 4.1, the results were obtained from several laws including Faradays Law, demonstrating the induced voltage of the linear alternator as in equation 4.1, stating that:

$$E_{induced} = -N\frac{d\emptyset}{dx} * \frac{dx}{dt} \tag{4.1}$$

However, equation (4.1.1) can further be simplified as follows:

$$E_{induced} = -N\frac{d\emptyset}{dt} \tag{4.2}$$

Figure 4.1 demonstrates velocity vs. time at maximum experiential frequency of approximately 40 Hz, in relation to the physical model frequency. The velocity of the translator is measured to gain insight into the difference in motion of the stator. Bearing in mind, the translator speed determines the system efficiency.

Figure 4.1 further demonstrates that there is both positive and negative motion throughout the duration of each cycle with a sinusoidal motion when compared to crankshaft driven pistons. Hence the service life of the crankshaft may be obtained by scaling and combining the magnitude and direction of the load [45]. The Free Piston Engine configuration is capable of achieving a desired compression ratio rapidly due to minimal moving parts [46].
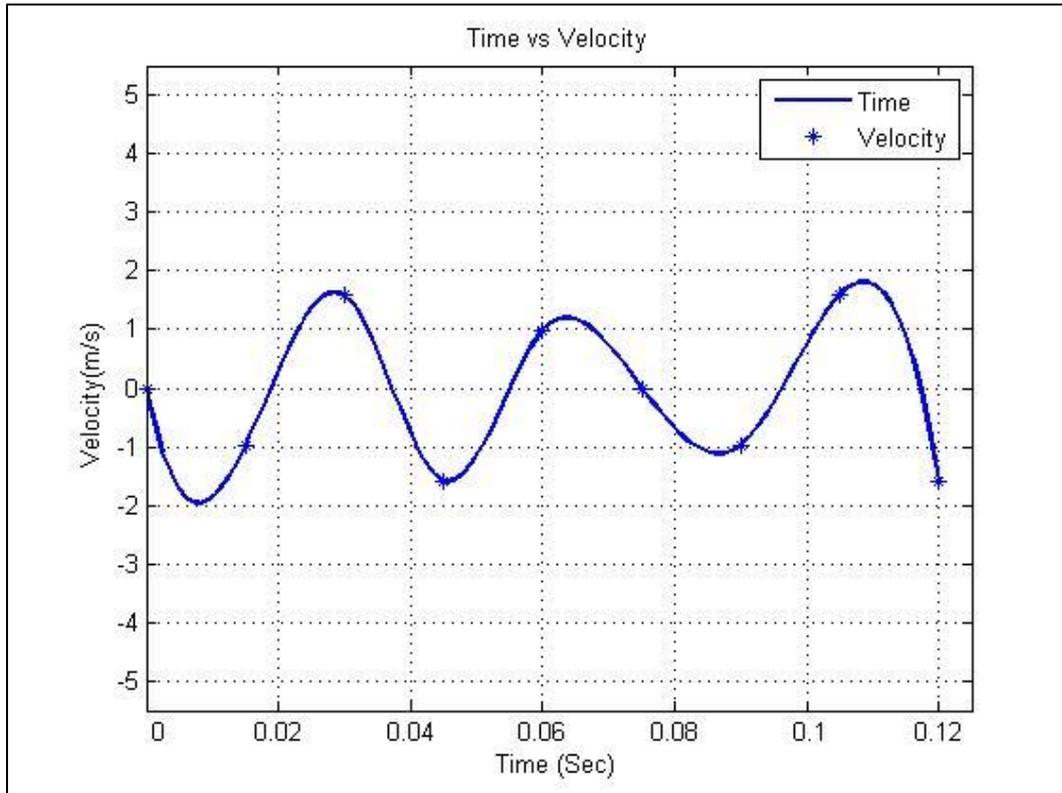
Figure 4.1: Simulated time vs velocity graph

In addition to Figure 4.1, current and power were simulated in order to determine the efficiency of the system, with respect to other another combustion engines and theoretical achievable system efficiency. It is with this approach that the piston operational speed is directly depended on the piston weight and as a result the induced voltage is proportional to the speed.

Figure 4.2, demonstrates the current that is generated by the generator during scavenging.

54
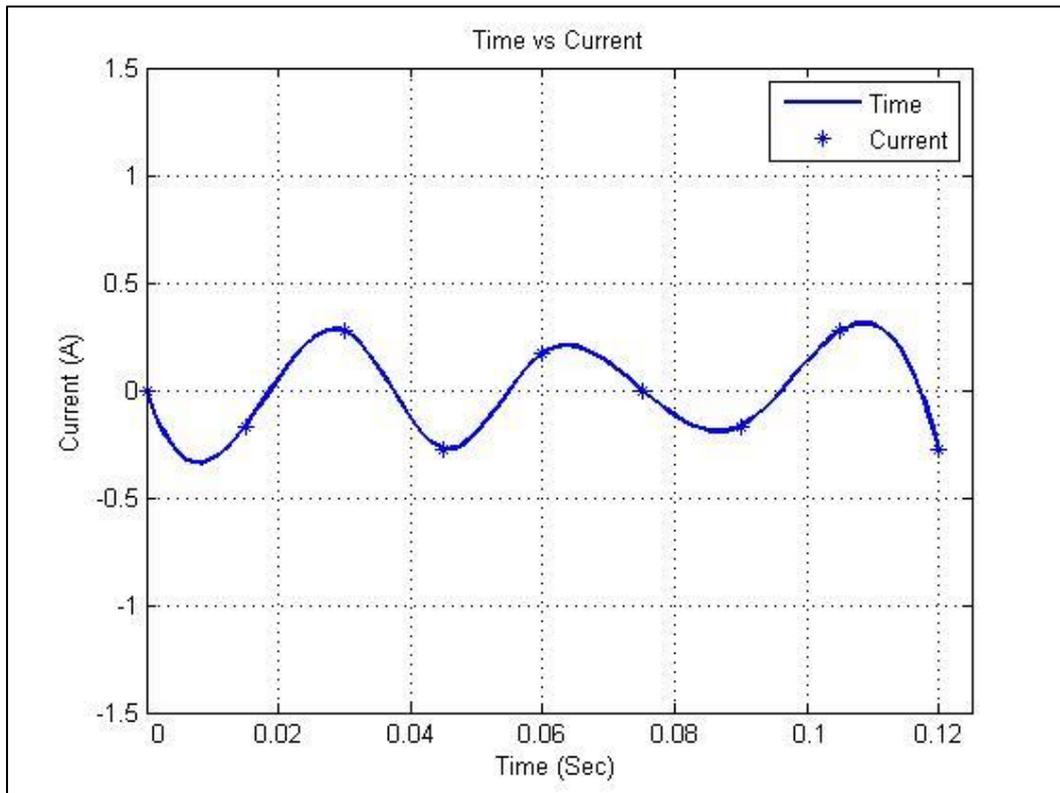
Figure 4.2: Simulated time vs current graph

The time vs. current graph indicated in Figure 4.2 through simulation highlights the *with-load* scenario. The simulation is obtained by changing a variable resistor from a high resistance to low resistance value. Figure 4.2 demonstrates the simulation at maximum load, in order to observe the maximum generated current of the system during scavenging at a fixed frequency of 40 Hz.

Since the tests are conducted in three states: *with load* (minimum resistance), *with-load at* maximum resistance *and without-load,* the maximum load testing was selected for current evaluation in Figure 4.2. Figure 4.2 further contributes to the power dissipation of the system at maximum load.

However, power is simulated in three other states namely: *with-load at* minimum, maximum load and no load for both the simulation and physical prototype.

4.3. Simulated Output Power and Operating Frequency

The engine resonant frequency relies on two aspects: *heat input and load*. The figure below presents the variation of the resonant frequency, after applying a load and further when the system heats up during scavenging, however, for this research, heat is not accounted for.

Annen at el.., [47], Hu at el.., [48], highlights the engine resonant frequencies in an existing Free Piston Engine, to operate from low frequencies of about 8.5 Hz to about 115 Hz. It is observed that Annen and Hus observations of low frequency usage in a generator model has advantages of higher output and minimal probability of damage in components such as coil. Figure 4.3 demonstrates the simulated output power obtained during testing as indicated in equation 4.3 below:

$$P_{out} = I^2 R_{max} \hspace{5cm} (4.3)$$

Where: P_{out} = Output power,

I^2 = generated current,

R_{max} = Maximum Resistance.
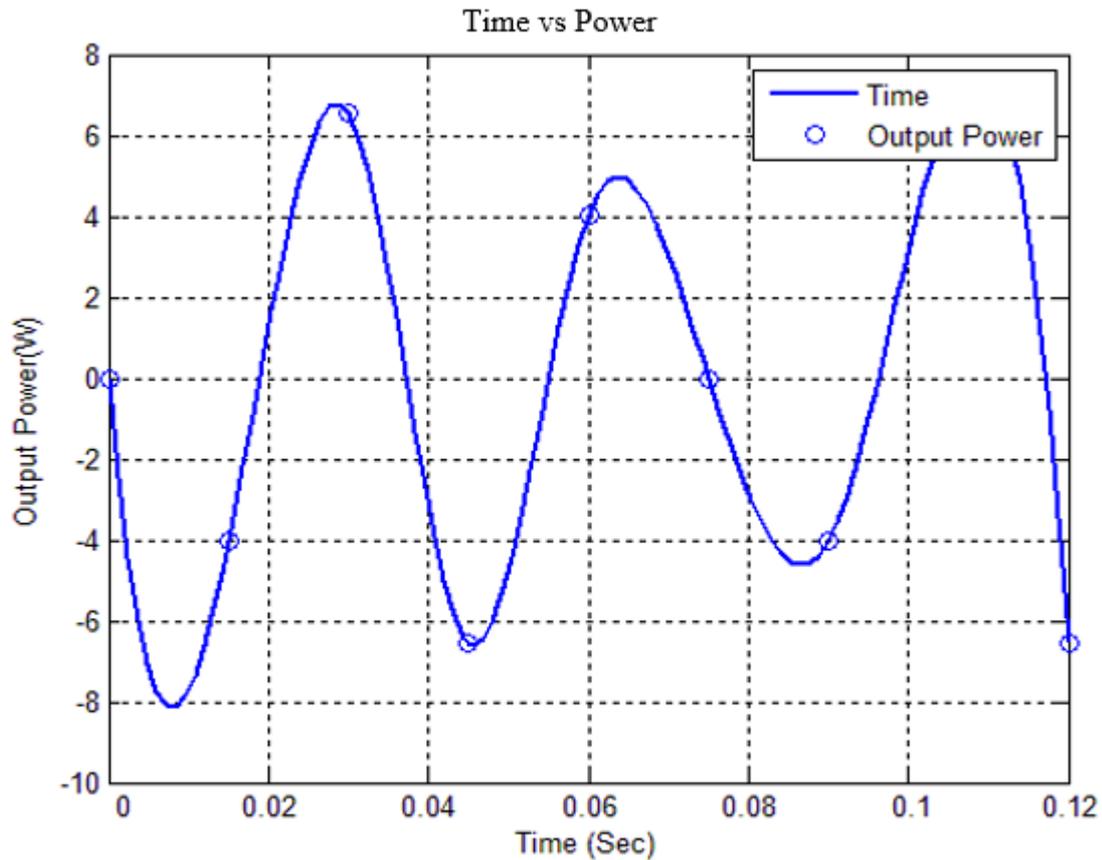
Figure 4.3: Simulated output power

The practicality of developing any system and simulation model may be determined by the accuracy in which they represent the actual system. The simulated output power is compared to the built system to verify the efficiency for both models, the combustion engine and the efficiency of the model.

Since flux is important for the purpose of this study, a workable conclusion was reached for the measure in magnetic flux density. For the physical model, the results were obtained for two states and compared to each other which are: with-load and without-load.

4.4.   Physical Model Output Results

The physical prototype results were evaluated as follows:

A variable high watt resistor was used to evaluate the linear generator output power at the with-load state. The output power evaluation was further varied to obtain results for both minimum and maximum resistance achievable by variable resistor.

The physical model represents the linear alternator in an engine. Figure 4.8 presents that the frequency of the physical model is higher than that of the simulation model. This is as a result of noise which causes signal distortion.

However, in order to reduce the noise, a filtering capacitor was introduced. The stroke-length of the built model is long as a result. This means that the compression ratio of the engine is higher than that of the simulation model.

Figure 4.6 represents the physical prototype output voltage at *with-load* stage. Ohms law is used to obtain the output power, as to compare the assembled generator efficiency to the theoretical engine results and the simulated results.

Figure 4.4, illustrates the output voltage at minimum *load* since a variable resistor is used.
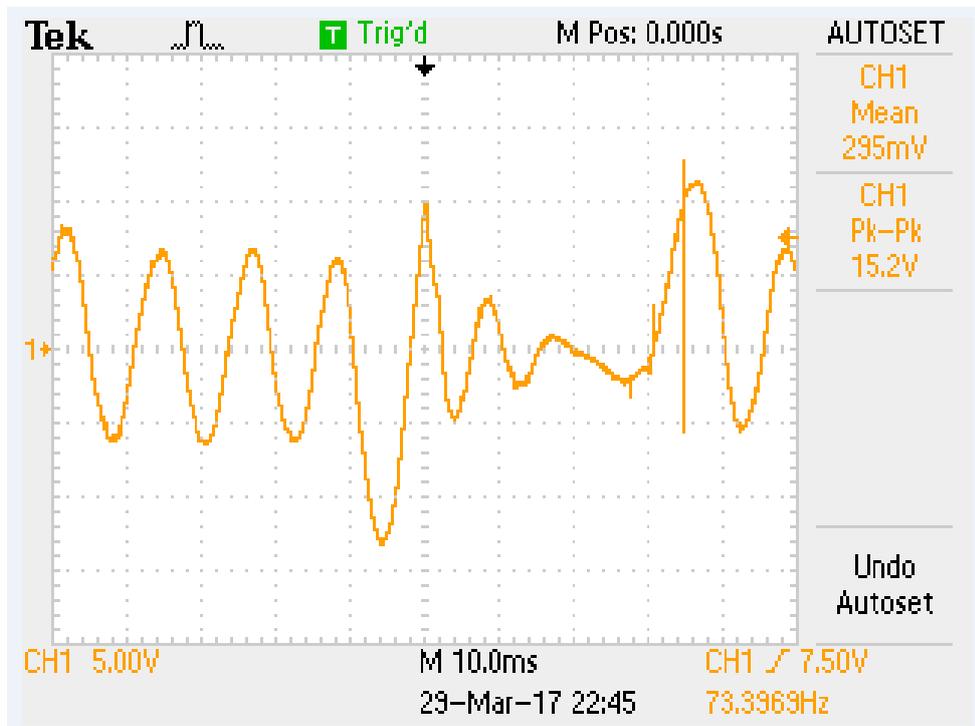
Figure 4.4: Output voltage at min load

58
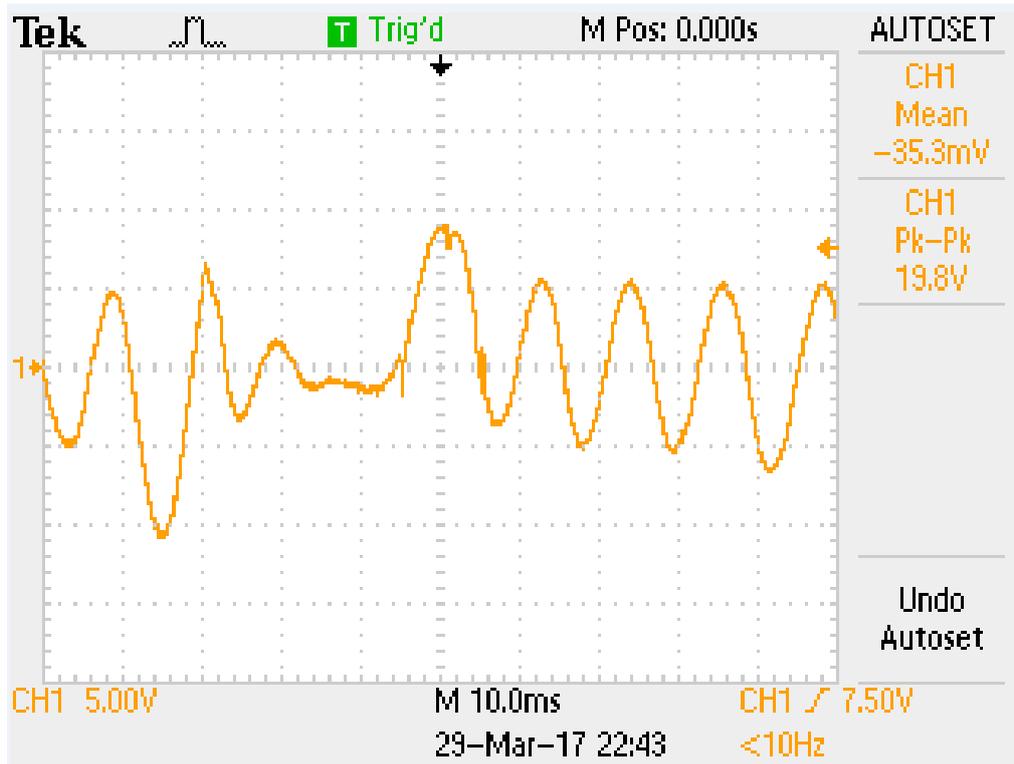
Figure 4.5: Output voltage at no load state

Figure 4.5, illustrates that the experimental results demonstrate a correlation between built and simulated results.

The physical model data as expressed in Figure 4.4 to Figure 4.6, demonstrates that frequency is indirectly proportional to the load, meaning that when the frequency decreases the load increases.

Figure 4.6 is obtained by adjusting the variable resistor to its maximum resistance. The functionality as well as the engine setup are set the same for all tests scenarios. Figure 4.5 demonstrates the output results for the *no-load* state.

59
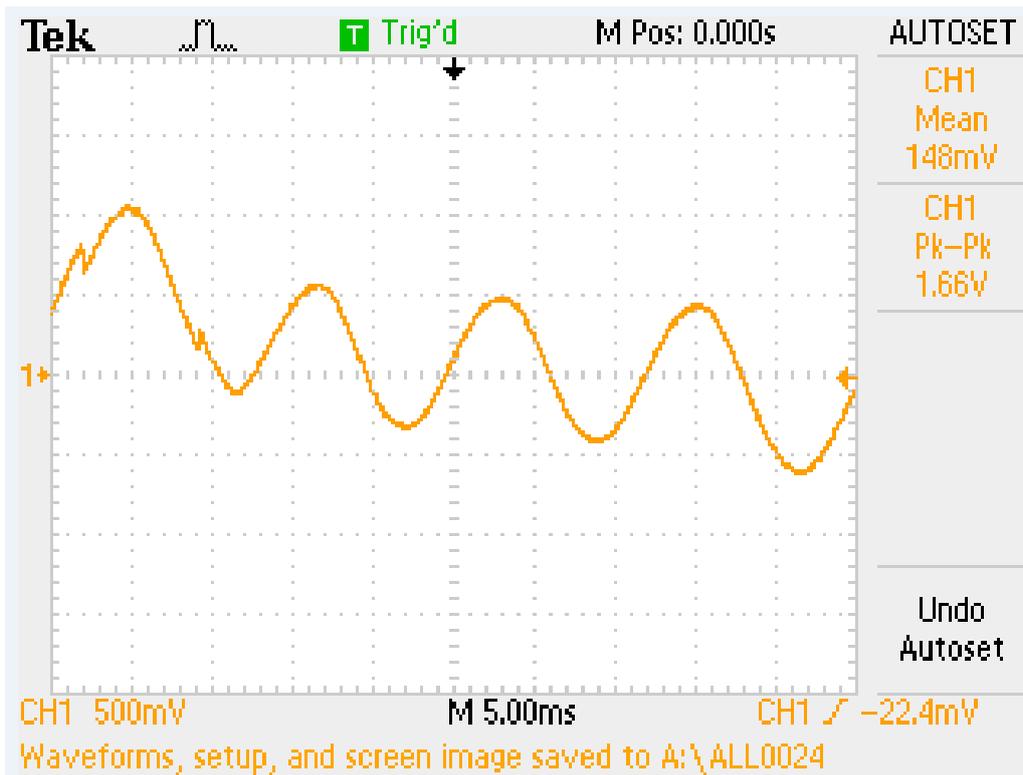
Figure 4.6: Output voltage at max load

The *no load* state during evaluation produced an output voltage of ~19.8V (p-p). The *with-load* states were further measured at both minimum and maximum resistance, producing voltage of about ~1.66V (p-p) for maximum resistance and 15.2V (p-p) for minimum resistance. Short computation duration of generating finite elements models are used for the above-mentioned results.

The magnetic flux is not only established from only permanent magnets, but also from the electric current in the coil, due to complexity of the electric current simulation.
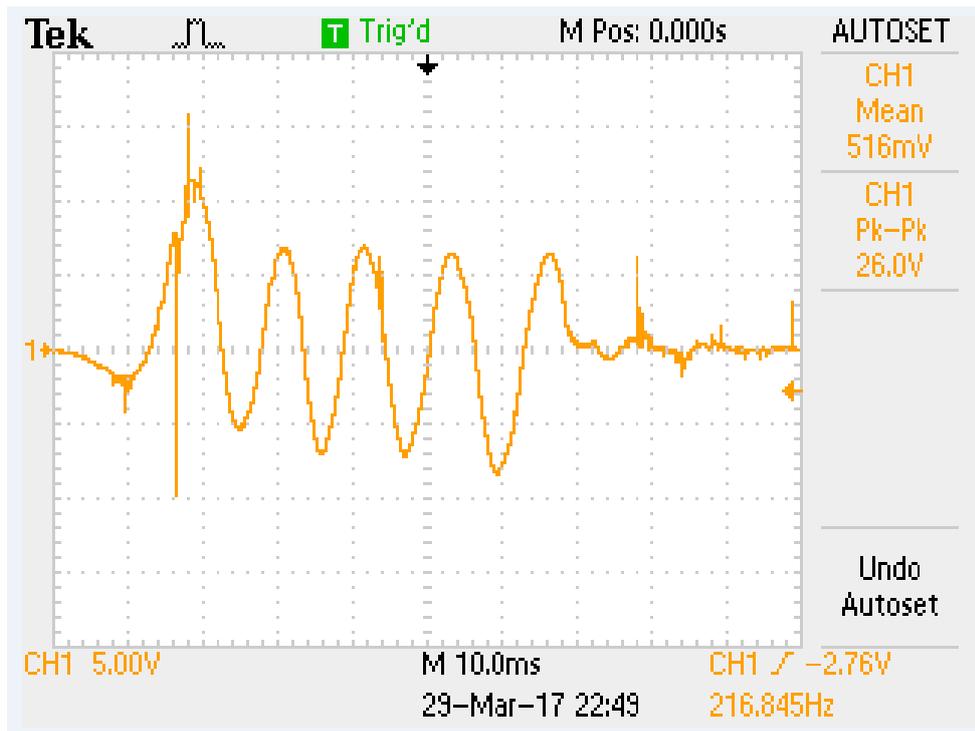
Figure 4.7: Output Voltage without Capacitor

The introduction of a capacitor in Figure 4.4 is to reduce noise that was observed in Figure 4.7. FPELG has lower noise to signal ratio and also maintain the frequency and operates at the standard appropriate frequency range highlighted by authors of Ref. 37 and Ref. 38.

The absence of the capacitor results in the system obtaining unstable frequency and noise. It is observed that the introduction of the capacitor brings stability in the system, as indicated in Figure 4.5. Equation 4.4 highlights the mathematical application with the introduction of the capacitor.

$$Emf = R_s i + L_s \frac{di}{dt} + \frac{1}{C} \int i \, dt + R_L i \tag{4.4}$$

Where:

R_s = Resistance,

i = Current,

L_s = Inductor,

C = Capacitor,

R_L = Load Resistor.

61

However, equation 4.5 can be simplified by adding both resistors (R_s and R_L), to obtain a total system resistance as follows;

$$R = R_s + R_L \qquad (4.5)$$

Therefore, equation (4.5) is simplified as follows:

$$Emf = Ri + L_s \frac{di}{dt} + \frac{1}{c} \int i dt \qquad (4.6)$$

However, due to high frequency, which in this case is 40 Hz, high capacitance is required to supress the voltage ripple within the linear generator as indicated in Figure 4.4 [49].

When the engine load is varied to maximum, an output voltage and frequency reduces rapidly to below 2 V (P-P).

Black: Linear Motor Frictional Losses (Simulated Model)
Orange: Linear Motor Frictional Losses (Physical Model)
Blue: Rotatory Motor frictonal Losses (Simulated Model)
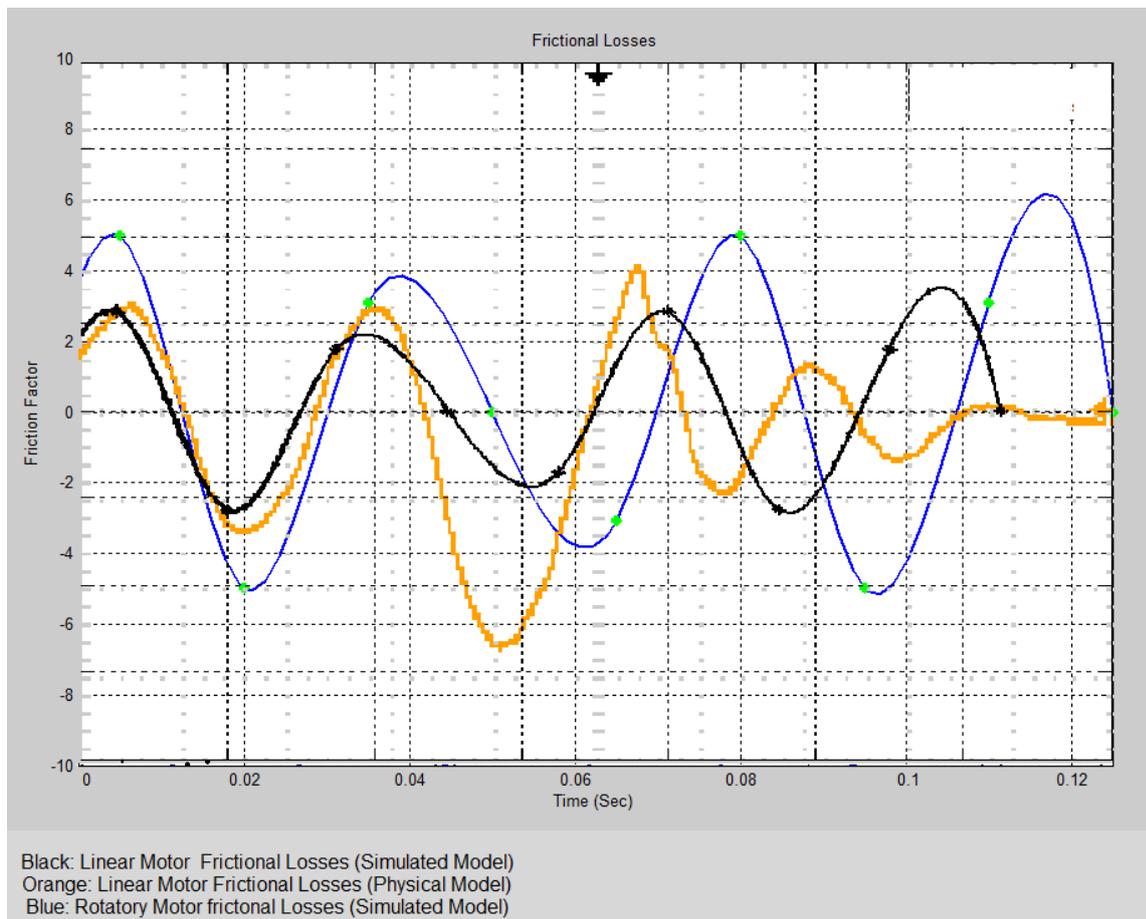
Figure 4 8: Frictional Losses on the tested generators

The models designed for both engine and alternators are accurately represented including Figure 4.7, illustrating the frictional losses. Figure 4.7 depicts the overall system efficiency, based on the frictional losses. Both the simulated and physical results are based on the '*no-load*' state, with FPELG having both the physical and simulated results. It is shown in Figure 4.7 that the system experienced further frictional losses on the simulated output, as compared to the physical model. However, the blue output wave with green dots presents the simulated crankshaft results, which in practice is expected to have higher losses compared to FPELG models.

However, the system efficiency is obtained through the use of the following equations:

$$\eta = \frac{P_{output}}{P_{assumed}} \qquad\qquad (4.7)$$

Where: P_{output} = Output Power,

$\qquad P_{assumed}$ = Output Power.

However, the output power was measured with reference to the copper power, since other forms of losses are ignored, a workable conclusion was reached to focus on copper.

Equation 4.8 highlights the output power with copper losses as indicated below:

$$P_{output} = P_{assumed} - P_{copper} - P_{copper\_loss} \qquad\qquad (4.8)$$

Where:

P_{copper} = copper power,

P_{copper_loss} = copper loss.

However, since friction and losses are not mainly accounted for in this research, merely ~ 10% of copper losses was accounted for.

63

4.5. Engine Comparison Results

The in-cylinder process for both the Free Piston Engine as well as the crankshaft engine are classified as being similar, hence, the efficiency parameters have been reported for Free Piston Engines by the following authors [50], [51].

In combustion engines, when the power output and spin rate increase, the losses due to friction account for a large portion of the engines gross output. As a result of frictional losses, a simulation model for mechanical losses and extrapolation from the known points is estimated as follows:

$$y(x) = y1 + \frac{x - x1}{x2 - x1}(y2 - y1) \tag{4.9}$$

It is debatable whether to directly separate piston friction from the rod friction [52]. However, since combustion engines are associated with friction, torque is always accounted for as follows:

$$f = \frac{2\pi NT}{T_s} \tag{4.10}$$

Where:

f = friction,

N = Speed,

T = Torque,

Ts = Total speed.

In [53], the authors highlight the frictional power losses for 41MPa and 70MPa at 2000rpm speed as follows:
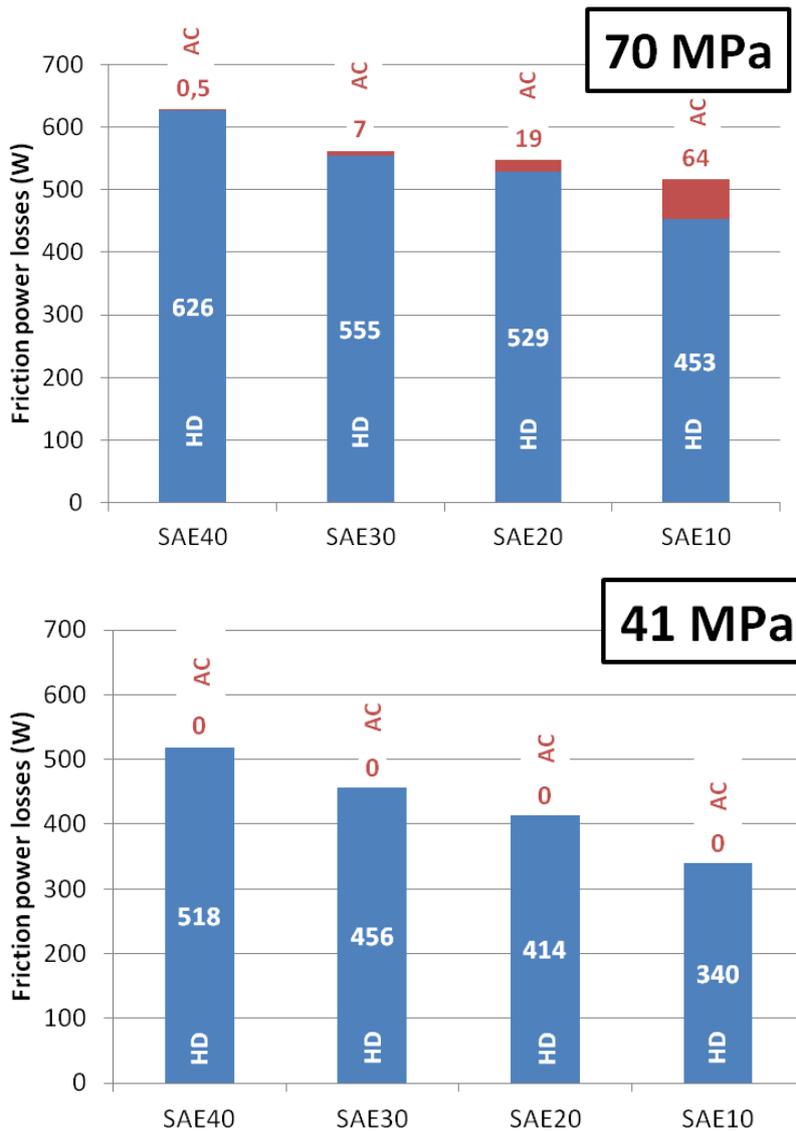
Figure 4.9: Comparison of the contributions to the friction power losses for a load of 70 MPa and 41 MPa

However, with reference to Figure 4.8, the results can be optimized to relate to the study with the supply air pressure of 6 bar, as indicated in Figure 4.9.

Since the supply air pressure is at 6 bars, then Ref [51] `s results may be recalculated as follows to meet the study requirements for fair power loss results.
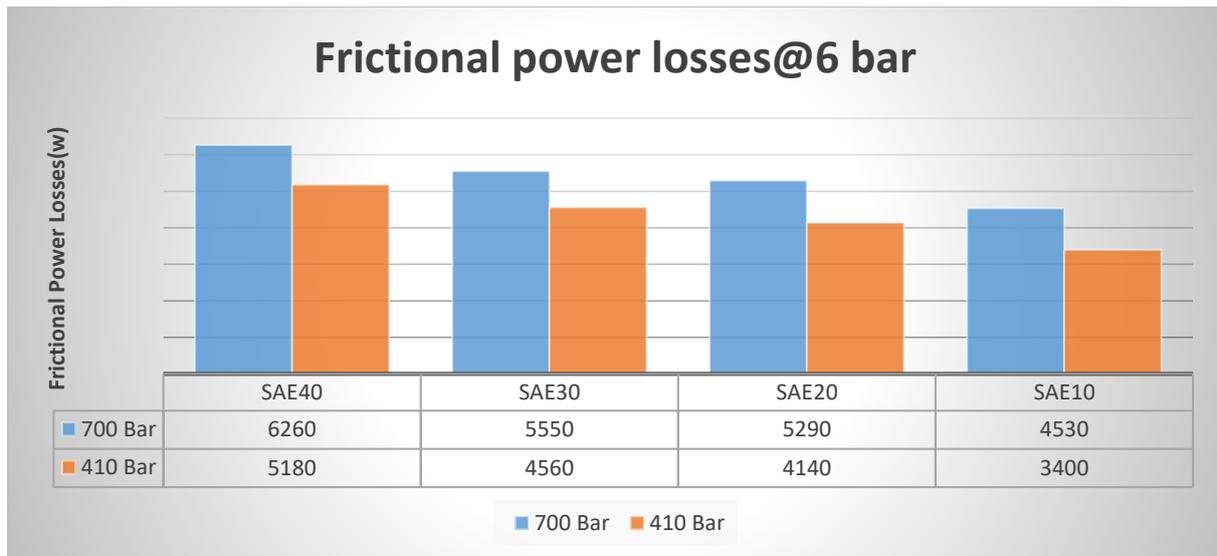
Figure 4.10: Frictional Power losses@6 bar

Figure 4.9, reflects the frictional losses calculated by authors of Ref [53]. However, Figure 4.9, underlines the frictional losses at 6 bars as indicated in equation 4.11 below.

The values on equation 4.11 are derived from Figure 4.8 above. The air pressure in Figure 4.8 is converted from MPa to Bar and from there the values are aligned to the 6 bar, which is the standardized air pressure used in this research.

From Figure 4.8, a ratio formula is utilized in order to obtain the frictional losses at 6 bars, as follows:

1 MPa = 10Bar.

As a result of the above ratio, SAE40 states that 626 (w) is achieved at 70MPa, however, since we are able to directly convert MPa to Bar, we will have an unknown variable x, used to obtain the frictional power loss for air pressure at 6 bars, as indicated in equation 4.11 below:

$$\frac{626}{x} = \frac{70}{700} \qquad (4.11)$$

However, advanced calculations approaches are the only means to completely exploit the potential development of the crankshaft and to ensure the component layout [54].

There are various kinds of losses associated with DC generators, as well as wind generators that may be compared to other forms of losses, associated with linear generators in addition to the authors of Ref [5]`s findings.

66
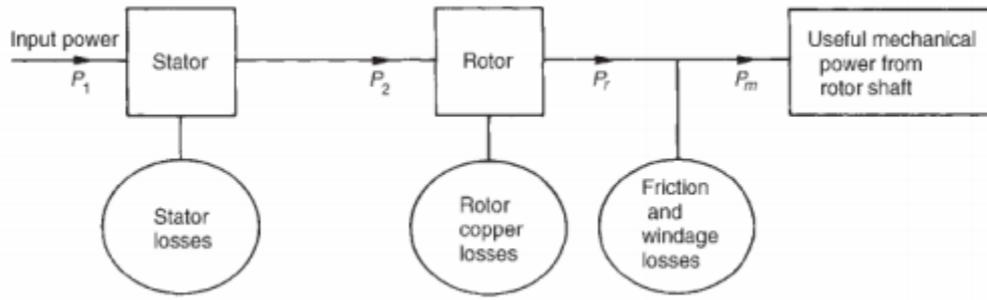
Figure 4 11: Power flow with associated losses during energy conversion *[55]*

Figure 4.10 underlines energy conversion methodology for a wind generator with different forms of losses, however, for this study solely bearing losses are accounted for.

In order to obtain the losses in this configuration, the mathematical formulas are derived from Ref [56], based on copper losses, as indicated in equation 4.12 below:

Copper losses are expressed as follows:

$$P_{cu\emptyset} = 3k_\emptyset R_{20°} I^2{}_{RMS}(W) \qquad (4.12)$$

Where:

$K_\emptyset$ = Temperature correction factor,

R_{20} = Phase Resistance,

I_{RMS} = Current

In addition to copper losses, iron losses are computed in accordance to Steinmetz equation:

$$P_{Fe} = k_h f B^\propto + \frac{k_e}{2\pi^2}(\frac{dB}{dt})^2 \qquad (4.13)$$

Where:

B = peak flux density,

$k_h, \propto, k_e$ = constants fitting on the manufacturers data.

However, as highlighted, bearing losses are the stand-alone losses that are accounted for in addition to verification or efficiency allocation of the generator.

According to [57], the mechanical losses are based on both frictional losses and windage losses, depending on the form of device constructed. However, for the present study, both

the frictional losses and windage losses are not accounted for as individual entities, but rather as two entities that contribute to mechanical losses, as indicated in equation 4.14 below:

$$P_{mec} = P_{fr} + P_{wind} \tag{4.14}$$

Where:

P_{mech} = Mechanical power,

P_{fr} = Frictional power,

P_{wind} = Wind power.

However, frictional bearings contributing to mechanical losses may be determined using the following formula:

$$P_{fr} = \frac{3}{2} N_r G_{rot} N * 10^{-3} \tag{4.15}$$

Where:

N_r is the bearing number,

G_{rot} is the rotor weight,

N is the speed.

In addition to frictional forces caused by the bearings, windage losses are also determined as follows:

$$P_{wind} = 2D^{3out} L N^3 * 10^{-6} \tag{4.16}$$

Where:

D_{out} = outer rotor diameter,

L = rotor length,

N = speed.

68

4.6.   Summary

In this chapter the free piston engine linear generator optimal operation model has been simulated in both Matlab$^{@}$ and physical prototype. The developed models have been successfully analysed in conjunction with study objectives and hypothesis as well as the cost used to develop the physical model. The Matlab$^{@}$/Simulink model were based on equations which were in line with the physical model specifications in order to conduct a fair efficiency evaluation between the two types of generators.

According to the results presentation on both models, it was observed that free piston engine linear generator is more efficient as compared to the combustion engine based on the output power ratio as well the frictional losses. It has been assumed that since both models are developed on the same test scale, the results obtained from either mathematical model or physical model will match the other model.

As a result, the developed optimal operation model has also been used to:

- Compare frictional losses between the free piston engine linear generator and the combustion engine.
- Evaluate the efficiency of crank-less linear generator.

Chapter 5: Conclusion

The main objective of this study was to design, develop, evaluate and simulate a form of linear alternator named Free Piston Engine Linear Generator. The linear generator designed was a 7W linear generator within a dual Free Piston Engine configuration. The engine was developed to combine both the linear alternator and piston engine to work as a single unit. In order to accomplish the above-mentioned objectives, the following tasks were completed.

Firstly, two methodologies had to be completed; an optimization program was developed for a 7W linear generator with velocity, current, voltage, output power and efficiency evaluation.

Secondly a physical model had to be developed, however, for the deliverance of quality results, the structural design was to be optimized to reduce frictional losses during scavenging.

It is concluded that the combustion engines experience further frictional losses compared to linear generators, due to mechanical wear, as well as the reduced amount of lubrication. However, since the translator is the only moving part in the Free Piston Engine Linear Generator, the engine is experiences frictional losses solely on the edges of the stator, due to the magnets and separator weight superseding the translator weight.

The frictional losses analysed were based on bearing losses in the combustion engines. The combustion engine frictional losses are interpreted using the simulated results, which in practice will be the same for the physical model.

5.1 System Development and Design

The dual free piston engine linear alternator developed was chosen, due to its simple configuration and fewer moving parts, as indicated in Chapter 2 and Chapter 3. Firstly, the structure was designed and developed with reference to the magnet size, since the efficiency is based on the linear motion during scavenging, as to minimize frictional losses.

70

Chapter 2 focuses on both Matlab$^{@}$/Simulink optimization program structure, as well as the parameters for developing the system (linear generator, free piston engine and the control system). The literature review behind free piston engine development and linear generator applications were highlighted.

The ideal structure and methodology for constructing the system were highlighted in Chapter 3 with reference to the objectives of the studies. However, in Chapter 3, it was established that the translator mass was less than that of the magnets combined with separators, since they are treated as one entity for the purpose of this study.

The load mass acting on the translator exceeds the translator as a result. The air pressure compensates for frictional losses. The translator balance references to the 40 Hz oscillating frequency. The frictional losses were experienced, however, solely the bearing losses are accounted for in this study.

In Chapter 4, the results for both models were presented, as a means of evaluating the efficiency of the linear alternator within a dual free piston engine configuration. Neodymium permanent magnets were attached to the translator with separators in between. The coil was attached to the stator as to allow the translator for scavenging. Furthermore, a variable resistor was used for the *with-load* scenario and was used to vary the results between the maximum and minimum resistance of the system.

The results of the engine simulation were compared to the physical prototype for the *with-load* scenario. It is observed that the simulation model is able to execute rapidly, as compared to the physical prototype, due to the fact that the simulation model is based on Matlab$^{@}$/Simulink algorithms.

Both models represented the accurate simulation results. However, the physical model is assumed as the feasible model, due to the fact that future work is aimed at developing the physical linear alternators model, ready for production.

Using the presented models, the system efficiency of the simulated linear generator was evaluated, with reference to the following output results:

- output current,
- velocity,
- output power with load,

71

- efficiency.

The above-mentioned results are based on the mathematical model. In addition to the results presented above, the physical prototype system efficiency was also evaluated, with reference to the following:

- output voltage at no load
- output voltage at minimum load
- output voltage at maximum load

It is observed that the mathematical model has higher amplitude compared to the physical model, which is a result of the air pressure force fading away below 6 bars, after a specific period of time on the physical model.

Since the system was tested both for minimum resistance and maximum resistance, the output power provides output power for both maximum and minimum resistance, as they are treated as one entity.

Furthermore, the output power is compared to the preliminary design output power. Finally, the optimum system model was obtained with adequate efficiency, limited mass, lower noise ratio and higher output power.

In retrospect to the objectives of this study, the following were achieved;

- To evaluate efficiency of linear based alternator in a free piston engine configuration, with an added necessity to develop a test benchmark.
- Using this setup and data generated scientifically to evaluate and compare the results to the Matlab$^{@}$/Simulink results were achieved.

The engine model used in this simulation accounts for engine speed. However, the engine speed was tested on the simulation model. As a result of these two tests, it is evident that the simulated output power and voltage are greater than that of the physical model, since the simulated results do not experience any form of frictional losses. The frictional losses that occur on the physical model contribute greatly to the frequency variation during the engine operation even though solely bearing frictional losses are considered for this study.

72

5.2. Suggested Future Work

The secondary objective of this research was to provide a foundation for future research in the field of power electronics and alternative energy (linear alternator design, evaluation analysis within a free piston engine configuration). This research further opens a window for further future research, such as the following:

- Cascading the generators and developing an ignition control unit that would make it possible to place it in production and scaling the output figures.
- Development of a three-phase alternator within a free piston engine configuration.

References

[1]   X. Wu, P. Jiang and J. Lu, "Multiagent-Based Distributed Load Shedding for Island Microgrids," pp. 6050-6062, 15 September 2014.

[2]   "Ministry of Economic Affairs, Agriculture and Innovation," [Online]. Available: http://www.government.nl/documents-and-publications/reports/2011/11/01/energy-report-2011.html. [Accessed 23 05 2017].

[3]   R. Mikalsen and A. P. Roskilly, "The Control of a Free-Piston engine generator. Part 1: fundamental analyses," vol. 87, p. 2, April 2010.

[4]   C. Y. Huang, C. K. Hu, C. j. Yu and C. K. Sung, "Experimental Investigation on the Perfomance of a Compressed Air Driven Piston," p. 1, 12 March 2013.

[5]   M. Goertz and L. Peng, "Free Piston Engine Its Application and optimization," in *FEV Engine Technology*, Detroit, Michigan, 2000.

[6]   T. A. Johnson, M. T. Leick and R. W. Moses, "Experimental Evaluation of the free piston engine linear alternator (FPLA)," p. 27, March 2015.

[7]   C. S. Hlang and H. Z. Myit, "Design analysis of a tubular type linear generator for free piston engine," vol. 3, p. 1, 08 May 2014.

[8]   N. Kumar , M. Hofacker and E. Barth, "Design and Control of a Free-Liquid-Piston Engine Compressor for Compact Robot Power," vol. 9, p. 1, 2013.

[9]   S. P. Koko, K. Kusakana and H. J. Vermaak, "Techno-Economic analysis of an off-grid micro hydro-kinetic river system as a remote rural area electrification option," Bloemfontein, Central University of Technology, Free-Sate, 2014, p. 20.

[10]   A. S. Zulkifli, M. N. Karsiti and A. Aziz, "Starting of a free-piston linear engine generator by mechanical resonance and rectangular current commutation," *Proceedings of the IEEE-Vehicle Power and Propulsion Conference,* pp. 1-7, 3-5 September 2008.

[11]   P. Famourie, W. R. Cawthorne, N. Clark, S. Nandkumar, C. Atkison, R. Atkison, T. McDaniel and S. Petreanu, "Design and Testing of a Novel Linear Alternator and Engine

system for Remote electric Power gneration," *" Proceedings of the IEEE Power Engineering Society Winter Meeting",* pp. 108-112, Feb 1999.

[12] R. Mikalsen and A. P. Roskilly, "The Control of a Free-Piston engine generator. Part 1: fundamental anaylyses," p. 1273, 4 August 2009.

[13] D. Petrichenko, Tatarnikov and I. Papkin , "Approach to electromagnetic Control of the extreme positions of a free piston generator," 2 December 2014.

[14] C. Ferrari and F. E. Hors, "Development of a free piston linear generator for use in an extended range electric vehicle," 6-9 May 2012.

[15] P. R. Guitart, "http://machinedesign.com/motorsdrives/how-calculate-new-dc-motor-parameters-modified-winding," Reliance Electric, 1 May 2000. [Online].

[16] M. Salman, "Analytic Design and Control aspect of a linear machine using co-simulation," p. 13, 2012.

[17] M. A. El-Refiae, "Fractional-Slot Concentrated-Windings Synchronous Permanent Magnet Machines," vol. 57, no. 1, pp. 107-121, Jan 2010.

[18] A. M. EL-Refaie and T. M. Jahns, "Optimal flux Weakening in Surface PM Machines Using Fractional-Slot Concentrated Windings," *IEEE Transactions on Industry Applications,* vol. 3, pp. 790-800, May 2005.

[19] P. Nemecek, M. Sindelka and O. Vysoky, "Ensuring Steady operation of Free-Piston Generator," vol. 4, no. 1, p. 19.

[20] Y. Miao, Z. Zuo, H. Feng, C. Guo, Y. Song, B. Jia and Y. Guo, "Research on the combustion characteristics of a Free-Piston Gasoline Engine Linear Generator during stable Generating process," p. 655, 18 August 2016.

[21] H. T. Aichlmayr, "Design Consideration, Modelling and analysis of Micro-Homogeneous charge Compression ignition combustion Free-Piston Engines," p. 28, December 2002.

[22] D.A Projects, [Online]. Available: http:diyaudioprojects.com/Technical/American-Wire-Gauge. [Accessed 14 September 2016].

[23] P. Kolpakhchyan, a. Kochin and a. Shaikhiev, "Emergency Generator design for the maritime transport based on the free piston combustion engine," p. 80, 24 April 2015.

[24] K. M. Zaseck, "Modeling and Control of hydraulic linear and free piston engines," p. 48, 2013.

[25] W. L. Mahadi, S. R. Adi and Wijo, "Application of ND2FE14B magnet in the linear generator," vol. 4, no. 2, p. 177, 2007.

[26] T. J. Callahan, "Free Piston Engine Linear Generator for Hybrid Vehicles Modeling Study," p. 10, May 1995.

[27] W. L. Wan Mahadi, S. R. Adi and K. M. Nor, "Thermal analysis of a neodymium iron boron (NDFEB) magnet in the linear generator design," p. 2, 26-29 September 2004.

[28] M. S. Azrin, "Modelling, Simulation and Implementation of Rectangular Commutation for Starting of Free-Piston Linear Generator," 2007.

[29] R. Szewczyk, "Validation of the Anhysteretic Magnetization Model for Soft Magnetic Materials with Perpendicular Anisotropy," p. 5115, 14 July 2014.

[30] "http://spontaneousmaterials.com/Papers/TN_0302," Arnold, the magnetic products group of SPS technologies, June 2003. [Online].

[31] W. Rodewald and M. Katter, "Properties and Applications of high performance magnets," [Online]. Available: http://www.vacuumschmelze.com/fileadmin/documents/pdf/fipublikationen/Paper_HPMA_2004_Magnets.pdf. [Accessed 02 June 2017].

[32] W. Rodewald and M. Katter, "Properties and Applications of high performance magnets," p. 3.

[33] W. R. Cawthorne, "Optimization of a brushless permanent magnet linear alternator for use with a linear internal combustion engine," Morgantown, West Virginia, 1999.

[34] "https://en.wikipedia.org/wiki/Crank_(mechanism)," Wikipedia, 13 09 2017. [Online].

[35] P. V. Blarigan, N. Paradiso and S. S. Goldsborough, "Homogeneous Charge Compression Ignition with a Free Piston," *A new Approach to Ideal Otto Cycle Performance, SAE International,* vol. 982484, 1998.

[36] S. Xu, Y. Wang, T. Zhu, T. Xu and C. Tao, "Numerical analysis of two-stroke free piston engine operating on HCCI combustion," vol. 88, pp. 3712-3725, 2011.

[37] "https://www.wolfram.com/mathematica/new-in-9/advanced-hybrid-and-differential-algebraic-equations/slider-crank-mechanism.html," [Online]. [Accessed 13 09 2017].

[38] F. Salazar, "Internal Combustion Engines," p. 62, 30 April 1998.

[39] S. Zulkifli, M. N. Karsiti and R. A. Aziz, "Starting of a Free-Piston Linear Engine Generator by Mechanical Resonance and Rectangular Current Commutation," p. 5, 3-5 September 2008.

[40] RS Components, [Online]. Available: http://docs-europe.electrocomponents.com/webdocs/133f/0900766b8133f933.pdf. [Accessed 30 11 2016].

[41] B. Jia, Z. Zuo, G. Tian, H. Feng and A. P. Roskilly, "Development and validation of a free-piston engine generator numerical model," p. 337, 28 November 2014.

[42] C. A. Oprea, L. Szabo and C. S. Martis, "Linear Permanent Magnet Electric Generator for Free Piston Engine Applications," 2012.

[43] J. Hansson, M. Leksell and F. Carlsson, "Minimizing Power Pulsations in a Free Piston Energy Converter".

[44] "htttps://www.mathworks.com/help/physmod/sdl/ref/pistonengine.html," [Online]. [Accessed 10 24 2017].

[45] F. H. Montazersadgh and A. Fatemi, "Stress analysis and Optimization of Crankshafts Subject to Dynamic Loading," 2007.

[46] P. V. Blarigan, "Advanced internal combustion electrical generator," p. 6, 2001.

[47] K. Annen, D. Sticker and J. Woodroffe, "Linearly oscillating miniature internal combustion (MICE) for portable electric power," *in 41st Aerospace Sciences Meeting and Exhibit.2003, AIAA Paper No.200-1113,* 2003.

[48] J. Hu, W. Wu, S. Yuan and C. Jing, "Mathematical modelling of a hydraulic free-piston engine considering hydralic valve dynamics, Energy," vol. 36, no. 10, pp. 6234-6242, October 2011.

[49] U. J. Seo, B. Riemer, R. Appunn and K. Hameyer, "Design considerations of a linear generator for a range extender application," Aachen, 2015.

[50] C. M. Atkinson, S. Petreanu, N. N. Clark, R. J. Atkinson, T. I. McDaniel, S. Nandkumar and P. Famourie, "Numerical Simulation of a Two-Stroke Linear Engine-Alternator Combination," *SAE International: Hybrid Vehicle Engines and Fuel Technology,* Vols. 1999-01-0921, 1999.

[51] P. V. Blarigan, N. Paradiso and S. S. Goldsborough, "Homogenous Charge compression Igntion with a Free Piston: A new Approach to Ideal Otto Cycle Performance," *SAE International,* vol. 982484, 1998.

[52] D. E. Richardson, "Review of Power Cylinder Friction for Diesel Engines," *ASME Journal of Engineering for Gas Turbines and Power 122,* pp. 506-519, 2000.

[53] H. Allmaier, C. Priestner, D. E. Sander and F. M. Reich, "Friction in Automotive Engines," p. 162, 2013.

[54] "cranktrain design optimized for reducing weight and friction supported by Coupled CAE Tools," p. 1.

[55] "UObabylon," 20 January 2018. [Online]. Available: http://www.uobabylon.edu.iq/uobColeges/ad_downloads/5_25878_628.pdf. [Accessed 5 October 2017].

[56] P. Andrada, M. Torrent, J. I. Perat and B. Blanque, "Power Losses in Outside-Spin Brushless D.C. Motors," vol. 1, no. 2, pp. 508-509, April 2004.

[57] J. F. Gieras and M. Wing, "Permanent Magnet Motor Technology, Design and Applications," 1997.

[58] U. J. Seo, B. Riemer, R. Appunn and K. Hameyer, "Design considerations of a linear generator for a range extender application," pp. 581-582, 2015.